Chapter | seven

Modeling Perturbed Relative Motion Using Orbital Elements

...And situated softly
Upon a pile of wind
Which in a perturbation
Nature had left behind.

Emily Dickinson (1830–1886)

Chapter 6 was devoted to orbital-element-based modeling of relative motion in unperturbed orbits. This chapter is organized into two parts. We begin with the presentation of analytical methods for propagating the perturbed relative motion variables via differential orbital elements and differential Euler parameters. These methods rely on the mean element propagation scheme outlined in Section 3.4 and constitute nonlinear theories. The second part of this chapter is devoted to linear theories including the STM of Gim and Alfriend (GA) and linear differential equation models for J_2-perturbed relative motion about mean circular orbits. A procedure for averaging the short-periodic corrections to the mean elements is discussed, leading to the development of *averaged orbital elements* and *averaged relative motion*. Finally, a more accurate, second-order state transition tensor is developed by incorporating quadratic nonlinearities of the two-body relative motion and the GA STM, which models the linearized J_2 effects.

7.1 THE UNIT-SPHERE APPROACH

The *unit-sphere approach*, as the name implies, projects the motion of the satellites in a formation onto a sphere of unit radius, allowing for application of the rules of spherical trigonometry. Such a projection uncouples from the motion of a satellite, the periodic variations of its radius due to the

Spacecraft Formation Flying; ISBN: 9780750685337

effects of eccentricity and other perturbations. The unit-sphere approach provides the projected relative motion coordinates and velocities without invoking any small-angle approximations. The solution, presented in terms of differential orbital elements, is exact and reveals the complex structure of the relative motion. The true or unscaled relative motion variables are obtained via re-scaling transformations from their scaled counterparts, involving the radii of the two satellites under consideration.

A satellite's motion can be projected onto a unit sphere by normalizing its Cartesian coordinates by its radius. The projection obtained thus is the sub-satellite point. The relative motion between two sub-satellite points is the focus of this section. Let C_0 and C_1 indicate the direction cosine matrices of the LVLH frames of the two satellites with respect to the ECI frame, $\mathscr{I}$. The relative position vector can be expressed in the rotating frame of the chief, $\mathscr{L}$, as follows (compare to our development in Section 6.1):

$$\begin{Bmatrix} \overline{x} \\ \overline{y} \\ \overline{z} \end{Bmatrix} = [C_0 C_1^T - I_3] \begin{Bmatrix} 1 \\ 0 \\ 0 \end{Bmatrix} \tag{7.1}$$

where $\overline{x}$, $\overline{y}$, and $\overline{z}$ are, respectively, the radial, in-track, and cross-track relative positions and I_3 stands for a 3×3 identity matrix. The direction cosine matrices can be parameterized by orbital elements. This allows for explicit solutions for the relative displacement variables in terms of the differential orbital elements as [124]

$$\begin{aligned}
\overline{x} = &-1 + \cos^2\frac{i_0}{2}\cos^2\frac{i_1}{2}\cos(\delta\theta + \delta\Omega) + \sin^2\frac{i_0}{2}\sin^2\frac{i_1}{2}\cos(\delta\theta - \delta\Omega) \\
&+ \sin^2\frac{i_0}{2}\cos^2\frac{i_1}{2}\cos(2\theta_0 + \delta\theta + \delta\Omega) \\
&+ \cos^2\frac{i_0}{2}\sin^2\frac{i_1}{2}\cos(2\theta_0 + \delta\theta - \delta\Omega) \\
&+ \frac{1}{2}\sin i_0 \sin i_1[\cos\delta\theta - \cos(2\theta_0 + \delta\theta)]
\end{aligned} \tag{7.2}$$

$$\begin{aligned}
\overline{y} = &\cos^2\frac{i_0}{2}\cos^2\frac{i_1}{2}\sin(\delta\theta + \delta\Omega) + \sin^2\frac{i_0}{2}\sin^2\frac{i_1}{2}\sin(\delta\theta - \delta\Omega) \\
&- \sin^2\frac{i_0}{2}\cos^2\frac{i_1}{2}\sin(2\theta_0 + \delta\theta + \delta\Omega) \\
&- \cos^2\frac{i_0}{2}\sin^2\frac{i_1}{2}\sin(2\theta_0 + \delta\theta - \delta\Omega) \\
&+ \frac{1}{2}\sin i_0 \sin i_1[\sin\delta\theta + \sin(2\theta_0 + \delta\theta)]
\end{aligned} \tag{7.3}$$

$$\overline{z} = -\sin i_0 \sin\delta\Omega\cos\theta_1 - [\sin i_0 \cos i_1 \cos\delta\Omega - \cos i_0 \sin i_1]\sin\theta_1 \tag{7.4}$$

Recall that the argument of latitude of the chief is $\theta_0 = \omega_0 + f_0$ and thus $\delta\theta$ indicates the differential argument of latitude. The radial and in-track variables involve the sum and difference of θ_0 and θ_1, since $2\theta_0 + \delta\theta = \theta_1 + \theta_0$ and $\delta\theta = \theta_1 - \theta_0$. On the other hand, $\overline{z}$ is an explicit function of θ_1 but not θ_0.

Hence, in general, the fundamental frequencies of the in-plane and cross-track motions are not the same.

Equations (7.2)–(7.4) are exact and valid for large angles. The effect of the J_2-perturbation can be studied by using osculating orbital elements in the above equations. However, one can also substitute expressions for the mean or averaged orbital elements [125], if desired, depending on the usage. The use of mean orbital elements and their secular drift rates, given in Eqs. (2.115), simplifies the process of the analytical propagation of relative motion considerably. However, Kepler's equation has to be solved to obtain a time-explicit solution. Eccentricity expansions for r and θ provide a time-explicit representation of the analytical solution without having to iterate on Kepler's equation. The equations for evaluating the mean drift rates are given below for the jth satellite in a formation:

$$\bar{\Omega}_j = \bar{\Omega}_j(0) + \dot{\bar{\Omega}}_j t \tag{7.5}$$

$$\bar{\omega}_j = \bar{\omega}_j(0) + \dot{\bar{\omega}}_j t \tag{7.6}$$

$$\bar{M}_j = \bar{M}_j(0) + \dot{\bar{M}}_j t \tag{7.7}$$

$$\dot{\bar{\Omega}}_j = -1.5 J_2 (R_e/\bar{p}_j)^2 \bar{n}_j \cos \bar{i}_j \tag{7.8}$$

$$\dot{\bar{\omega}}_j = 0.75 J_2 (R_e/\bar{p}_j)^2 \bar{n}_j \left(5\cos^2 \bar{i}_j - 1\right) \tag{7.9}$$

$$\dot{\bar{M}}_j = \bar{n}_j \left[1 + 0.75 J_2 \sqrt{1-\bar{e}_j^2} (R_e/\bar{p}_j)^2 \left(3\cos^2 \bar{i}_j - 1\right)\right] \tag{7.10}$$

$$\bar{n}_j = \sqrt{\frac{\mu}{\bar{a}_j^3}} \tag{7.11}$$

Note that henceforth M_0 will indicate the mean anomaly of the chief. The mean elements can be converted into the respective osculating elements via the Brouwer transformation [66].

The dimensional relative motion variables are obtained from their unit-sphere counterparts by re-scaling, as shown below:

$$x = r_1(1+\overline{x}) - r_0 \tag{7.12}$$

$$\begin{Bmatrix} y \\ z \end{Bmatrix} = r_1 \begin{Bmatrix} \overline{y} \\ \overline{z} \end{Bmatrix} \tag{7.13}$$

$$\dot{x} = r_1 \dot{\overline{x}} + \dot{r}_1(1+\overline{x}) - \dot{r}_0 \tag{7.14}$$

$$\begin{Bmatrix} \dot{y} \\ \dot{z} \end{Bmatrix} = r_1 \begin{Bmatrix} \dot{\overline{y}} \\ \dot{\overline{z}} \end{Bmatrix} + \dot{r}_1 \begin{Bmatrix} \overline{y} \\ \overline{z} \end{Bmatrix} \tag{7.15}$$

Note that the unit-sphere expressions for the in-track and cross-track motion variables are scaled versions of the respective physical coordinates; the scaling factor is the radius of the deputy (not that of the chief). The relative velocity states can be obtained by differentiating Eqs. (7.2)–(7.4) with respect to time.

Equations (7.2)–(7.4) can be simplified for small differential elements via linearization and the resulting solutions for the motion variables can be

expressed as

$$x = r_1 - r_0 \tag{7.16}$$

$$y = r_1(\delta\theta + \delta\Omega \cos i_0) \tag{7.17}$$

$$z = r_1(-\sin i_0 \delta\Omega \cos\theta_1 + \delta i \sin\theta_1) \tag{7.18}$$

It is also reasonable for many applications to approximate r_1 and θ_1 in Eqs. (7.17)–(7.18) by r_0 and θ_0, respectively. A higher-order approximation for relative motion with respect to near-circular orbits has been devised by Hill et al. [126], based on the COWPOKE (Cluster Orbits with Perturbation of Keplerian Elements) model, originally developed by Sabol et al. [127]. The differential elements δM, $\delta\Omega$, and $\delta\omega$ are assumed large in this model, and a first-order eccentricity expansion for f is employed. The relative position coordinates are given by

$$x = \frac{(a_0 + \delta a)[1 - (e_0 + \delta e)^2]}{1 + (e_0 + \delta e)\cos(M_0 + 2e_0 \sin M_0 + \delta f)} - \frac{a_0(1 - e_0^2)}{1 + e_0 \cos f} \tag{7.19}$$

$$y = r_0(\delta\theta + \delta\Omega \cos i_0) \tag{7.20}$$

$$z = r_0 \left[-2 \sin i_0 \sin\left(\frac{\delta\Omega}{2}\right) \cos\left(M_0 + \omega_0 + 2e_0 \sin M_0 + \frac{\delta\theta}{2}\right) + \delta i \sin(M_0 + \omega_0 + 2e_0 \sin M_0 + \delta\theta) \right] \tag{7.21}$$

where

$$\delta M = \delta M(0) + \left[\sqrt{\frac{\mu}{(a_0 + \delta a)^3}} - \sqrt{\frac{\mu}{a_0^3}} \right] t \tag{7.22}$$

and

$$\delta f = \delta M + 2(e_0 + \delta e)\sin(M_0 + \delta M) - 2e_0 \sin M_0 \tag{7.23}$$

The COWPOKE equations have been found useful for cluster analysis of GEO satellites.

A method based on the numerical integration of the GVE, incorporating the disturbances due to J_2, differential atmospheric drag, and differential solar radiation pressure has been presented by Balaji and Tatnall [128]. The relative motion states are obtained from the perturbed osculating orbital elements of the satellites using an approach similar to the unit-sphere procedure.

If the periodic variations in y are neglected, then we can write

$$y \approx \bar{a}_0(\delta\bar{\lambda} + \delta\bar{\Omega} \cos\bar{i}_0) \tag{7.24}$$

The derivative of the above approximation can be obtained from the secular drift rates of Eqs. (7.8)–(7.10) and thus an *along-track boundedness condition*

can be derived:

$$\dot{y} \approx \bar{a}_0(\delta\dot{\bar{\lambda}} + \delta\dot{\bar{\Omega}}\cos\bar{i}_0) = 0 \tag{7.25}$$

This condition results in a constraint on $\delta\bar{a}$, as will be shown in Chapter 8, to mitigate an adverse effect of J_2. An independent derivation of this result, valid for circular orbits, is presented in Eq. (7.140).

7.2 RELATIVE MOTION DESCRIPTION USING QUATERNIONS

The direction cosine matrices in Eq. (7.1) can also be parameterized by two quaternions – sets of Euler parameters – as discussed in Section 2.4 and as shown by Junkins and Turner [129], one each for the chief and the deputy. The applications of this analogy to the determination of relative attitude is discussed in Chapter 9. A closely-related parametrization in terms of the Kustaanheimo–Stiefel variables is given in Ref. [54]. As shown in Section 2.4, the quaternion of a satellite's LVLH frame can be related to its orbital elements as:

$$\begin{aligned} \beta_0 &= \cos\frac{i}{2}\cos\frac{\Omega+\theta}{2} \quad & \beta_1 &= \sin\frac{i}{2}\cos\frac{\Omega-\theta}{2} \\ \beta_2 &= \sin\frac{i}{2}\sin\frac{\Omega-\theta}{2} \quad & \beta_3 &= \cos\frac{i}{2}\sin\frac{\Omega+\theta}{2} \end{aligned} \tag{7.26}$$

Equations (7.26), adapted from Ref. [54], can be used to obtain the quaternion via the mean element propagation scheme. The quaternion description is nonsingular. For example, i and Ω can be set to zero for an equatorial orbit.

The direction cosine matrix representing the rotation from ECI to the LVLH frame associated with a satellite can be parameterized in terms of its quaternion as (cf. also the discussion in Section 2.4)

$$C = \begin{bmatrix} \beta_0^2+\beta_1^2-\beta_2^2-\beta_3^2 & 2(\beta_1\beta_2+\beta_0\beta_3) & 2(\beta_1\beta_3-\beta_0\beta_2) \\ 2(\beta_1\beta_2-\beta_0\beta_3) & \beta_0^2-\beta_1^2+\beta_2^2-\beta_3^2 & 2(\beta_2\beta_3+\beta_0\beta_1) \\ 2(\beta_1\beta_3+\beta_0\beta_2) & 2(\beta_2\beta_3-\beta_0\beta_1) & \beta_0^2-\beta_1^2-\beta_2^2+\beta_3^2 \end{bmatrix} \tag{7.27}$$

Given the quaternion for the orbit of a satellite at any instant, its unit radius vector can be obtained from Eq. (7.27) as

$$\hat{\mathbf{r}} = \begin{bmatrix} \beta_0^2+\beta_1^2-\beta_2^2-\beta_3^2 & 2(\beta_1\beta_2+\beta_0\beta_3) & 2(\beta_1\beta_3-\beta_0\beta_2) \end{bmatrix}^T \tag{7.28}$$

The quaternion propagation equation is

$$\begin{Bmatrix} \dot{\beta}_0 \\ \dot{\beta}_1 \\ \dot{\beta}_2 \\ \dot{\beta}_3 \end{Bmatrix} = \frac{1}{2}\begin{bmatrix} 0 & -\omega_x & -\omega_y & -\omega_z \\ \omega_x & 0 & \omega_z & -\omega_y \\ \omega_y & -\omega_z & 0 & \omega_x \\ \omega_z & \omega_y & -\omega_x & 0 \end{bmatrix}\begin{Bmatrix} \beta_0 \\ \beta_1 \\ \beta_2 \\ \beta_3 \end{Bmatrix} \tag{7.29}$$

It is well known (cf. Eqs. (7.143b) and (7.150b)) that the osculation constraint results in $\omega_y = 0$.

Relative orientation of the LVLH frame of the deputy with respect to that of the chief can be expressed by a relative quaternion using a finite rotation [29]:

$$\begin{Bmatrix} \delta\beta_0 \\ \delta\beta_1 \\ \delta\beta_2 \\ \delta\beta_3 \end{Bmatrix} = \begin{bmatrix} \beta_{01} & \beta_{11} & \beta_{21} & \beta_{31} \\ \beta_{11} & -\beta_{01} & -\beta_{31} & \beta_{21} \\ \beta_{21} & \beta_{31} & -\beta_{01} & -\beta_{11} \\ \beta_{31} & -\beta_{21} & \beta_{11} & -\beta_{01} \end{bmatrix} \begin{Bmatrix} \beta_{00} \\ \beta_{10} \\ \beta_{20} \\ \beta_{30} \end{Bmatrix} \tag{7.30}$$

where the second subscript on the quaternions refers to a particular satellite, either the chief or deputy. The elements of the relative quaternion vector can be explicitly obtained by substituting Eqs. (7.26) for the chief and deputy into Eq. (7.30) as

$$\begin{aligned} \delta\beta_0 &= \cos\frac{i_0}{2}\cos\frac{i_1}{2}\cos\left(\frac{\delta\theta+\delta\Omega}{2}\right) + \sin\frac{i_0}{2}\sin\frac{i_1}{2}\cos\left(\frac{\delta\theta-\delta\Omega}{2}\right) \\ \delta\beta_1 &= -\sin\frac{i_0}{2}\cos\frac{i_1}{2}\cos\left(\frac{\delta\theta+\delta\Omega}{2}\right) + \cos\frac{i_0}{2}\sin\frac{i_1}{2}\cos\left(\frac{\delta\theta-\delta\Omega}{2}+\theta_0\right) \end{aligned} \tag{7.31a}$$

$$\begin{aligned} \delta\beta_2 &= \sin\frac{i_0}{2}\cos\frac{i_1}{2}\sin\left(\frac{\delta\theta+\delta\Omega}{2}+\theta_0\right) - \cos\frac{i_0}{2}\sin\frac{i_1}{2}\sin\left(\frac{\delta\theta-\delta\Omega}{2}+\theta_0\right) \\ \delta\beta_3 &= \cos\frac{i_0}{2}\cos\frac{i_1}{2}\sin\left(\frac{\delta\theta+\delta\Omega}{2}\right) + \sin\frac{i_0}{2}\sin\frac{i_1}{2}\sin\left(\frac{\delta\theta-\delta\Omega}{2}\right) \end{aligned} \tag{7.31b}$$

The relative position of the deputy with respect to the chief can be written very simply by noting that $C_0C_1^T$ in Eq. (7.1) is nothing but the relative direction cosine matrix for a rotation from the deputy's LVLH frame onto that of the chief. Hence, it follows from Eqs. (7.27) and (7.28) that

$$\begin{Bmatrix} \overline{x} \\ \overline{y} \\ \overline{z} \end{Bmatrix} = \begin{Bmatrix} (\delta\beta_0^2 + \delta\beta_1^2 - \delta\beta_2^2 - \delta\beta_3^2) - 1 \\ 2(\delta\beta_1\delta\beta_2 + \delta\beta_0\delta\beta_3) \\ 2(\delta\beta_1\delta\beta_3 - \delta\beta_0\delta\beta_2) \end{Bmatrix} = 2\begin{Bmatrix} -(\delta\beta_2^2 + \delta\beta_3^2) \\ \delta\beta_1\delta\beta_2 + \delta\beta_0\delta\beta_3 \\ \delta\beta_1\delta\beta_3 - \delta\beta_0\delta\beta_2 \end{Bmatrix} \tag{7.32}$$

The position variables $(1+\overline{x})$, $\overline{y}$, and $\overline{z}$ can be interpreted as the three direction cosines of the unit radius vector of the deputy with respect to the LVLH frame of the chief. Therefore, the following relationship exists between the three relative position variables:

$$(1+\overline{x})^2 + \overline{y}^2 + \overline{z}^2 = 1 \tag{7.33}$$

Furthermore, $\overline{x} \leq 0$.

Focusing attention on $\overline{y}$ in Eq. (7.32), it is observed that for small formations, the term $\delta\beta_1\delta\beta_2$ is at least an order of magnitude smaller than $\delta\beta_0\delta\beta_3$. Hence, under the mentioned assumption, an excellent approximation for the in-track

relative position is given by

$$\overline{y} \approx 2\delta\beta_3 \tag{7.34}$$

Similarly, for small formations

$$\overline{z} \approx -2\delta\beta_2 \tag{7.35}$$

The influence of the differential quaternion on $\overline{x}$ is of second order.

The relative quaternion can be propagated directly from the kinematic relationship

$$\begin{Bmatrix} \delta\dot{\beta}_0 \\ \delta\dot{\beta}_1 \\ \delta\dot{\beta}_2 \\ \delta\dot{\beta}_3 \end{Bmatrix} = \frac{1}{2} \begin{bmatrix} 0 & -\delta\omega_x & -\delta\omega_y & -\delta\omega_z \\ \delta\omega_x & 0 & \delta\omega_z & -\delta\omega_y \\ \delta\omega_y & -\delta\omega_z & 0 & \delta\omega_x \\ \delta\omega_z & \delta\omega_y & -\delta\omega_x & 0 \end{bmatrix} \begin{Bmatrix} \delta\beta_0 \\ \delta\beta_1 \\ \delta\beta_2 \\ \delta\beta_3 \end{Bmatrix} \tag{7.36}$$

with the differential angular velocity vector obtained from

$$\begin{Bmatrix} \delta\omega_x \\ \delta\omega_y \\ \delta\omega_z \end{Bmatrix} = \begin{Bmatrix} \omega_{x1} \\ \omega_{y1} \\ \omega_{z1} \end{Bmatrix} - C_1 C_0^T \begin{Bmatrix} \omega_{x0} \\ \omega_{y0} \\ \omega_{z0} \end{Bmatrix} \tag{7.37}$$

The matrix product $C_1 C_0^T$ in Eq. (7.37) can be evaluated as the direction cosine matrix for a rotation from the LVLH frame of the chief onto that of the deputy, i.e., it can be obtained by substituting the elements of the differential quaternion into Eq. (7.27). Furthermore, as noted previously, the osculating orbit constraint results in $\omega_{y0} = \omega_{y1} = 0$.

The remaining angular velocities and the radius of each satellite can be evaluated using the orbital equations of motion written in its own LVLH frame:

$$\ddot{r} - {\omega_z}^2 r = -\frac{\mu}{r^2} + u_x + d_x \tag{7.38a}$$

$$r\dot{\omega}_z + 2\dot{r}\omega_z = u_y + d_y \tag{7.38b}$$

$$r\omega_x\omega_z = u_z + d_z \tag{7.38c}$$

where the components of the control and J_2 disturbance vectors included are as defined in Eqs. (5.7)–(5.9). The components of the J_2 disturbing acceleration vector can be obtained by evaluating the gradient of $\mathcal{R}$ defined in Section 2.5.3 as

$$\mathbf{d} = \begin{Bmatrix} d_x \\ d_y \\ d_z \end{Bmatrix} = -\frac{3}{2}\frac{J_2 \mu R_e^2}{r^4} \begin{Bmatrix} 1 - 3\sin^2 i \sin^2\theta \\ \sin^2 i \sin 2\theta \\ \sin 2i \sin\theta \end{Bmatrix} \tag{7.39}$$

Equation (7.39) can be represented in terms of the Euler parameters with the help of the following identities:

$$\sin i \sin\theta = 2\left(\beta_1\beta_3 - \beta_0\beta_2\right) \tag{7.40a}$$

$$\cos i = \left(1 - 2\beta_1^2 - 2\beta_2^2\right) \tag{7.40b}$$

$$\sin i \cos\theta = 2\left(\beta_0\beta_1 + \beta_2\beta_3\right) \tag{7.40c}$$

Finally, we obtain

$$\mathbf{d} = -\frac{3}{2}\frac{J_2\mu R_e^2}{r^4}\begin{Bmatrix} 1 - 12\left(\beta_1\beta_3 - \beta_0\beta_2\right)^2 \\ 8\left(\beta_1\beta_3 - \beta_0\beta_2\right)\left(\beta_0\beta_1 + \beta_2\beta_3\right) \\ 4\left(1 - 2\beta_1^2 - 2\beta_2^2\right)\left(\beta_0\beta_1 + \beta_2\beta_3\right) \end{Bmatrix} \tag{7.41}$$

In summary, a complete nonlinear simulation with quaternions can be performed by utilizing Eq. (7.29) and Eqs. (7.38a)–(7.38c) for the chief and deputy. Relative motion variables can be extracted from the results of numerical integration using Eqs. (7.12)–(7.15), (7.30), and (7.32). Alternatively, Eq. (7.36) can be simulated instead of Eq. (7.29) to obtain the relative quaternion of the deputy. The total number of differential equations for this nonsingular approach is 14. The number of equations can be reduced by two with the use of $\beta_0 = \sqrt{(1 - \beta_1^2 - \beta_2^2 - \beta_3^2)}$. Gurfil [50] presents the LPE for the quaternion elements subjected to the J_2-perturbation as an alternative approach to a singularity-free simulation; see also Eqs. (2.116).

We have discussed nonlinear methods for the analytical propagation of the relative motion dynamics. Attention is focused on linear methods of propagation in the subsequent sections of this chapter.

7.3 THE GIM–ALFRIEND GEOMETRIC METHOD

The purpose of this section is to derive the state transition matrices for both osculating and mean elements for the relative motion of two neighboring satellites when the reference satellite (chief) is in an elliptic orbit, and both satellites are subjected to the J_2 perturbation. The linear differential equations of relative motion for this system are formidable. A perturbation solution in powers of J_2 could probably be obtained, but there is an easier approach. Rather than solving the equations of motion, the approach is to use the geometric relationship between the relative state and the orbital elements for the two satellites, similarly to the rationale discussed in Chapter 6. If one has the orbital elements for the two objects, then the relative state can be obtained, and vice versa. This approach was used by Garrison [130] to obtain a solution for the relative motion assuming a spherical Earth. With this approach, solving the differential equations of relative motion can be avoided. Since this approach uses the geometric relationship between the relative state and orbital elements, it is referred to as the *Geometric Method* (GM).

7.3.1 J_2 effects revisited

As we have seen in Sections 2.6, 3.4 and 7.1, the gravitational perturbations create secular, short-periodic and long-periodic variations of the orbital elements, where the long-periodic terms have a frequency equal to the perigee rotation rate. In Chapter 5, when assuming a spherical Earth, we showed that to avoid unnecessary fuel expenditure, the chief orbit's eccentricity should be included in the dynamical model through the Lawden or the Tschauner–Hempel equations (instead of the CW equations).

Rewriting Eqs. (7.8)–(7.10), we obtain the mean angle rates subject to a J_2 perturbation:

$$\begin{aligned} n &= \bar{n} + 0.75 J_2 \bar{n} \left(\frac{R_e}{p}\right)^2 \eta \left(2 - 3\sin^2 i\right) \\ \dot{\Omega} &= -1.5 J_2 \bar{n} \left(\frac{R_e}{p}\right)^2 \cos i \\ \dot{\omega} &= -0.75 J_2 \bar{n} \left(\frac{R_e}{p}\right)^2 \left(1 - 5\cos^2 i\right) \end{aligned} \tag{7.42}$$

where

$$p = a\eta^2, \quad \eta = \left(1 - e^2\right)^{1/2} \tag{7.43}$$

and $\bar{n}$ is the mean motion for the unperturbed orbit. A difference in the semimajor axis, eccentricity or inclination of the satellites in a formation can cause a difference in the secular rates of the two objects, resulting in secular drift. This is in contrast to the spherical Earth problem, in which only a semimajor axis difference can cause secular drift, and only in the along-track direction. Note that only e^2, not e, appears in the secular rate equations. Thus, it is the difference in e^2 that causes the secular drift. This means that for near-circular orbits, the effect of a change in the eccentricity will be much smaller than the effect of a comparable change in inclination. However, for highly eccentric orbits, such as the NASA MMS mission discussed in Section 1.7, the effect of a change in eccentricity can be comparable to the effect of a change in inclination. The differential secular effects are obtained by a Taylor series expansion about the chief's orbit; for an inclination change they are:

$$\delta n = \delta \dot{l} = -\left[4.5 J_2 \bar{n} \left(\frac{R_e}{p_0}\right)^2 \eta_0 \sin i_0 \cos i_0\right] \delta i \tag{7.44}$$

$$\delta \dot{\Omega} = \left[1.5 J_2 \bar{n} \left(\frac{R_e}{p_0}\right)^2 \sin i_0\right] \delta i \tag{7.45}$$

$$\delta \dot{\omega} = -\left[7.5 J_2 \bar{n} \left(\frac{R_e}{p_0}\right)^2 \sin i_0 \cos i_0\right] \delta i \tag{7.46}$$

Example 7.1. *Determine the differential secular effects over one orbit for a chief circular orbit of* 7000 km*, an inclination of* 70° *and a differential inclination that results in an out-of-plane motion of* 1 km*, that is,* $\delta i = 1/7000$ rad.

The differential effects are

$$\delta l = -\left[9J_2\pi\left(\frac{R_e}{a_0}\right)^2 \sin i_0 \cos i_0\right]\left(\frac{1}{a_0}\right) \tag{7.47}$$

$$\delta\Omega = \left[3J_2\pi\left(\frac{R_e}{a_0}\right)^2 \sin i_0\right]\left(\frac{1}{a_0}\right) \tag{7.48}$$

$$\delta\omega = -\left[15J_2\pi\left(\frac{R_e}{a_0}\right)^2 \sin i_0 \cos i_0\right]\left(\frac{1}{a_0}\right) \tag{7.49}$$

The along-track drift is $a_0(\delta l + \delta\omega + \delta\Omega\cos i_0) = -19$ m and the cross-track drift is $a_0\delta\Omega \sin i_0 = 7.5$ m. Since the along-track drift per orbit is $= -3\pi\delta a$, if the J_2 effects are not modeled, the control system would interpret this drift as a semimajor axis error of approximately 2.02 m and correct for it. However, once the control action is complete, the J_2 effects would start the drift again. Thus, if the secular J_2 effects are not included in the dynamic model, fuel will be wasted. It will be shown later that this along-track drift can be negated with a small change in semimajor axis.

Now, let us consider the case of a leader–follower formation with a mean eccentricity of zero and determine the relative motion. Using the equations in Appendices D, E and F we get

$$\delta\bar{\theta} = \delta\bar{\theta}(t_0) \tag{7.50}$$

$$\delta\theta = \left[1 - J_2R_e^2\left(D_{22}^{(sp1)} + D_{22}^{(sp2)}\right)\right]\delta\bar{\theta} \tag{7.51}$$

$$\delta\Omega = -J_2R_e^2\left(D_{62}^{(sp1)} + D_{62}^{(sp2)}\right)\delta\bar{\theta} \tag{7.52}$$

$$a_0 = \bar{a}_0 + a^{(sp1)} + a^{(sp2)} \tag{7.53}$$

$$\bar{q}_{10} = \bar{q}_{20} = 0 \tag{7.54}$$

$$q_{10} = \left(q_1^{(sp1)} + q_1^{(sp2)}\right) \tag{7.55}$$

$$q_{20} = \left(q_2^{(sp1)} + q_2^{(sp2)}\right) \tag{7.56}$$

$$r_0 = a_0/\left(1 + q_{10}\cos\theta_0 + q_{20}\sin\theta_0\right) \tag{7.57}$$

$$y = \bar{a}_0\left[1 - \frac{17}{4}J_2\left(\frac{R_e}{\bar{a}_0}\right)^2 \sin^2\bar{i}_0\cos 2\bar{\theta}_0\right]\delta\bar{\theta} \tag{7.58}$$

$$a = \bar{a}_0\left[1 + \frac{9}{4}J_2\left(\frac{R_e}{\bar{a}_0}\right)^2\left(1 - 3\cos^2\bar{i}_0\right)\right] \tag{7.59}$$

Example 7.2. *Evaluate the along-track drift for a chief satellite orbit with* $\bar{a}_0 = 7000$ km, $\bar{i}_0 = 70°$ *and a separation of* 1 km*, so that* $\delta\bar{\theta} = 1/7000$ rad.

Using Eq. (7.58) we obtain

$$y = \left[1 - 0.0041\cos(2\bar{\theta}_0)\right] \text{ km} \tag{7.60}$$

Thus, there is an along-track oscillation of approximately 4 meters. Whether or not the short-periodic terms should be included in the dynamical model will depend on the preciseness of the required control. If CDGPS is used for the relative navigation, it will provide a relative position error of several centimeters (cf. Chapter 12), so this oscillatory motion will certainly be detected. Over a short period of time, it will resemble a secular drift if it is not included in the dynamical model. The type of control system, the size of the control box and the type of formation will determine whether or not the short-periodic terms need to be included in the dynamic model (a high-fidelity formation flying simulation is discussed in Chapter 13). At a minimum, these terms should be evaluated to determine what effect they may have. For example, in the current problem if the control box was set at ±3 m then the control system would continually be negating the natural short-periodic oscillations. This would not be wise, if it is avoidable.

This analysis has shown that there is a need for a dynamical model that includes the absolute and differential J_2 effects in addition to the chief orbit's eccentricity. In response to this need, the next subsection derives a state transition matrix that is valid for any eccentricity, and includes the first-order absolute and differential J_2 effects.

7.3.2 The geometric method

Let the relative state of the deputy be $\mathbf{x} = (x, \dot{x}, y, \dot{y}, z, \dot{z})^T$, and the chief orbital elements be $\mathbf{\alpha e} = (a, \theta, i, q_1, q_2, \Omega)^T$, where θ is the argument of latitude, $q_1 = e\cos\omega$, and $q_2 = e\sin\omega$. This nonsingular set, defined in Section 2.4, is used because the true anomaly and the argument of perigee are undefined for a circular orbit. After obtaining the orbital elements of the deputy by a Taylor series expansion about the orbital elements of the chief, the differential orbital elements between them are obtained by $\delta\mathbf{\alpha e} = \mathbf{\alpha e}_1 - \mathbf{\alpha e}_0$.

In the subsequent discussion, we will use the following notation convention: All the orbital elements without subscript are related to the chief, and $\mathbf{x}$ and $\delta\mathbf{\alpha e}$ are related to the deputy. To obtain more accurate results, a curvilinear coordinate system, $\mathscr{C}$, represented by unit vectors $(\hat{\mathbf{x}}, \hat{\mathbf{y}}, \hat{\mathbf{z}})$ with the origin at the chief, is used instead of the LVLH Cartesian frame $\mathscr{L}$; see our discussion in Section 5.5. Thus, x is the difference in the radii, and y and z are the curvilinear distances along the imaginary circular orbit on the reference orbital plane and perpendicular to the reference orbit, respectively, as shown in Fig. 7.1. The equivalent deputy-fixed curvilinear coordinate system will be denoted by $\mathscr{D}$.

Using the osculating elements for the chief and the deputy under the influence of J_2, and the total angular velocity $\boldsymbol{\varpi} = \dot{\theta}\hat{\mathbf{x}} + \dot{\Omega}\hat{\mathbf{k}} + \mathrm{d}i/\mathrm{d}t\left(\cos\theta\hat{\mathbf{x}} - \sin\theta\hat{\mathbf{y}}\right)$,

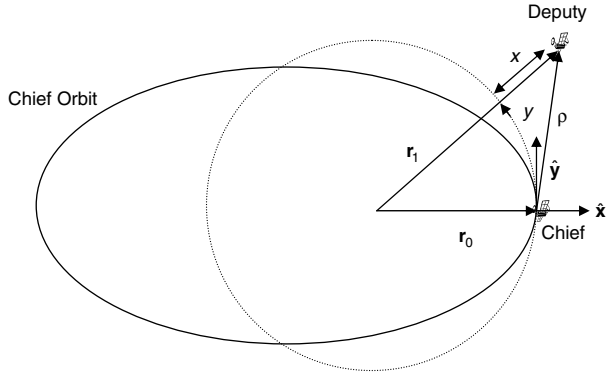

FIGURE 7.1 Curvilinear coordinate system.

where $(\hat{\mathbf{i}}, \hat{\mathbf{j}}, \hat{\mathbf{k}})$ are unit vectors in the ECI reference frame, $\mathscr{I}$, the geometric transformation between $\mathbf{x}(t)$ and $\delta\boldsymbol{\alpha}(t)$ is represented by

$$\mathbf{x}(t) = [A(t) + A_2 B(t)]\,\delta\boldsymbol{\alpha}(t) \tag{7.61}$$

where $A_2 = 3J_2R_e^2$, R_e is the equatorial radius of the Earth, and the matrix B contains only the terms perturbed by J_2. Let $\phi_{\boldsymbol{\alpha}}$ be the state transition matrix for the relative osculating elements, that is, $\delta\boldsymbol{\alpha}(t) = \phi_{\boldsymbol{\alpha}}\delta\boldsymbol{\alpha}(t_0)$. Therefore, from the solution, $\mathbf{x}(t) = \Phi_{J_2}(t, t_0)\mathbf{x}(t_0)$, the state transition matrix for the relative motion, $\Phi_{J_2}(t, t_0)$, is

$$\Phi_{J_2}(t, t_0) = [A(t) + A_2 B(t)]\,\phi_{\boldsymbol{\alpha}}(t, t_0)\,[A(t_0) + A_2 B(t_0)]^{-1} \tag{7.62}$$

Let $\overline{\boldsymbol{\alpha}}$ represent the mean elements, and $\boldsymbol{\alpha}$ represent the instantaneous, or osculating, elements. Using the transformation matrix $D(t)$, transforming from the relative mean elements to the relative osculating elements (see Appendix F), and the state transition matrix $\bar{\phi}_{\overline{\boldsymbol{\alpha}}}(t, t_0)$ for the relative mean elements, we can write

$$\delta\boldsymbol{\alpha}_{osc}(t) = D(t)\delta\overline{\boldsymbol{\alpha}}(t) = D(t)\bar{\phi}_{\overline{\boldsymbol{\alpha}}}(t, t_0)\delta\overline{\boldsymbol{\alpha}}(t_0) \tag{7.63}$$

where

$$D(t) = \frac{\partial\boldsymbol{\alpha}}{\partial\overline{\boldsymbol{\alpha}}} \tag{7.64}$$

$\Phi_{J_2}(t, t_0)$ becomes

$$\begin{aligned}\Phi_{J_2}(t, t_0) = {} & [A(t) + A_2 B(t)]\,D(t)\bar{\phi}_{\overline{\boldsymbol{\alpha}}}(t, t_0)D^{-1}(t_0) \\ & \times [A(t_0) + A_2 B(t_0)]^{-1}\end{aligned} \tag{7.65}$$

The state transition matrix for the mean elements is

$$\bar{\Phi}_{J_2}(t, t_0) = \left[\bar{A}(t) + A_2\bar{B}(t)\right]\bar{\phi}_{\overline{\boldsymbol{\alpha}}}(t, t_0)\left[\bar{A}(t_0) + A_2\bar{B}(t_0)\right]^{-1} \tag{7.66}$$

Since the mean and osculating elements are equal when $J_2 = 0$, $\bar{A}(t) = A(t)$. The angular velocities for the mean and osculating elements are different, consequently, $\bar{B}(t) \neq B(t)$.

THE TRANSFORMATION MATRIX $\Sigma(t) = [A(t) + A_2B(t)]$

The approach used here is to express the position and velocity of the deputy in terms of the relative state and differential orbital elements and equate the two. The position and velocity of the chief and deputy are

$$\mathbf{r}_0 = r_0\hat{\mathbf{x}} \tag{7.67}$$

$$\mathbf{v}_0 = \dot{r_0}\hat{\mathbf{x}} + r_0\varpi_{n0}\hat{\mathbf{y}} - r_0\varpi_{t0}\hat{\mathbf{z}} \equiv v_{r0J_2}\hat{\mathbf{x}} + v_{t0J_2}\hat{\mathbf{y}} + v_{n0J_2}\hat{\mathbf{z}} \tag{7.68}$$

$$\mathbf{r}_1 = \mathbf{r}_0 + \boldsymbol{\rho} = (r_0 + x)\,\hat{\mathbf{x}} + y\hat{\mathbf{y}} + z\hat{\mathbf{z}} \tag{7.69}$$

$$\mathbf{v}_1 = (v_{r0J_2} + \dot{x} - y\varpi_{n0} + z\varpi_{t0})\hat{\mathbf{x}} + \left(v_{t0J_2} + \dot{y} + x\varpi_{n0} - z\varpi_{r0}\right)\hat{\mathbf{y}} \tag{7.70}$$

$$+ \left(v_{n0J_2} + \dot{z} - x\varpi_{t0} + y\varpi_{r0}\right)\hat{\mathbf{z}} \tag{7.71}$$

where the subscript J_2 means that the velocity components include the effects of J_2, and

$$\boldsymbol{\varpi} \equiv \varpi_r\hat{\mathbf{x}} + \varpi_t\hat{\mathbf{y}} + \varpi_n\hat{\mathbf{z}} \tag{7.72}$$

The position and velocity vectors of the deputy can also be obtained in curvilinear coordinates by using a Taylor series expansion about the chief and the geometric transformation. The deputy's position in the chief orbit reference frame is given by

$$[\mathbf{r}_1]_{\mathscr{C}} = T_{\mathscr{J}}^{\mathscr{C}}T_{\mathscr{D}}^{\mathscr{J}}[\mathbf{r}_1]_{\mathscr{D}} \tag{7.73}$$

where $T_{\mathscr{J}}^{\mathscr{C}}$ and $T_{\mathscr{D}}^{\mathscr{J}}$ are the coordinate transformations between the chief and inertial frame and the inertial and deputy orbit frames, respectively. The transformation from an orbit frame $\mathscr{O}$, representing either frame $\mathscr{C}$ or $\mathscr{D}$, and the inertial frame $\mathscr{J}$, is given by

$$\begin{aligned} T_{\mathscr{J}}^{\mathscr{O}} &= \begin{pmatrix} \mathrm{c}_\theta & \mathrm{s}_\theta & 0 \\ -\mathrm{s}_\theta & \mathrm{c}_\theta & 0 \\ 0 & 0 & 1 \end{pmatrix}\begin{pmatrix} 1 & 0 & 0 \\ 0 & \mathrm{c}_i & \mathrm{s}_i \\ 0 & -\mathrm{s}_i & \mathrm{c}_i \end{pmatrix}\begin{pmatrix} \mathrm{c}_\Omega & \mathrm{s}_\Omega & 0 \\ -\mathrm{s}_\Omega & \mathrm{c}_\Omega & 0 \\ 0 & 0 & 1 \end{pmatrix} \\ &= \begin{pmatrix} \mathrm{c}_\theta\mathrm{c}_\Omega - \mathrm{s}_\theta\mathrm{c}_i\mathrm{s}_\Omega & \mathrm{c}_\theta\mathrm{s}_\Omega + \mathrm{s}_\theta\mathrm{c}_i\mathrm{c}_\Omega & \mathrm{s}_\theta\mathrm{s}_i \\ -\mathrm{s}_\theta\mathrm{c}_\Omega - \mathrm{c}_\theta\mathrm{c}_i\mathrm{s}_\Omega & -\mathrm{s}_\theta\mathrm{s}_\Omega + \mathrm{c}_\theta\mathrm{c}_i\mathrm{c}_\Omega & \mathrm{c}_\theta\mathrm{s}_i \\ \mathrm{s}_i\mathrm{s}_\Omega & -\mathrm{s}_i\mathrm{c}_\Omega & \mathrm{c}_i \end{pmatrix} \end{aligned} \tag{7.74}$$

where, as before, we used the compact notation $\mathrm{c}_x \equiv \cos x$ and $\mathrm{s}_x \equiv \sin x$. Now we expand Eq. (7.73) in a Taylor series about the chief satellite's motion:

$$[\mathbf{r}_1]_{\mathscr{C}} = T^{\mathscr{C}}_{\mathscr{I}} \left(T^{\mathscr{I}}_{\mathscr{C}} + \delta T^{\mathscr{I}}_{\mathscr{C}} \right) \begin{pmatrix} r_0 + \delta r \\ 0 \\ 0 \end{pmatrix}$$

$$[\mathbf{r}_1]_{\mathscr{C}} = \begin{pmatrix} r_0 \\ 0 \\ 0 \end{pmatrix} + r_0 T^{\mathscr{C}}_{\mathscr{I}} \begin{pmatrix} \delta T^{\mathscr{C}}_{\mathscr{I}\,11} \\ \delta T^{\mathscr{C}}_{\mathscr{I}\,12} \\ \delta T^{\mathscr{C}}_{\mathscr{I}\,13} \end{pmatrix} \tag{7.75}$$

The δT_{ij} are

$$\delta T^{\mathscr{C}}_{\mathscr{I}\,11} = T^{\mathscr{C}}_{\mathscr{I}\,21}\delta\theta - T^{\mathscr{C}}_{\mathscr{I}\,12}\delta\Omega + \left(T^{\mathscr{C}}_{\mathscr{I}\,13} \sin\Omega_0 \right) \delta i \tag{7.76}$$

$$\delta T^{\mathscr{C}}_{\mathscr{I}\,12} = T^{\mathscr{C}}_{\mathscr{I}\,22}\delta\theta + T^{\mathscr{C}}_{\mathscr{I}\,11}\delta\Omega - \left(T^{\mathscr{C}}_{\mathscr{I}\,13} \cos\Omega_0 \right) \delta i \tag{7.77}$$

$$\delta T^{\mathscr{C}}_{\mathscr{I}\,13} = T^{\mathscr{C}}_{\mathscr{I}\,23}\delta\theta + (\sin\theta_0 \cos i_0)\, \delta i \tag{7.78}$$

$$\delta T^{\mathscr{C}}_{\mathscr{I}\,21} = -T^{\mathscr{C}}_{\mathscr{I}\,11}\delta\theta - T^{\mathscr{C}}_{\mathscr{I}\,22}\delta\Omega + T^{\mathscr{C}}_{\mathscr{I}\,23} \sin\Omega_0 \delta i \tag{7.79}$$

$$\delta T^{\mathscr{C}}_{\mathscr{I}\,22} = -T^{\mathscr{C}}_{\mathscr{I}\,12}\delta\theta + T^{\mathscr{C}}_{\mathscr{I}\,21}\delta\Omega - T^{\mathscr{C}}_{\mathscr{I}\,23} \cos\Omega_0 \delta i \tag{7.80}$$

$$\delta T^{\mathscr{C}}_{\mathscr{I}\,23} = -T^{\mathscr{C}}_{\mathscr{I}\,13}\delta\theta + (\cos\theta_0 \cos i_0)\, \delta i \tag{7.81}$$

$$\delta T^{\mathscr{C}}_{\mathscr{I}\,31} = -T^{\mathscr{C}}_{\mathscr{I}\,32}\delta\Omega + (\cos i_0 \sin\Omega_0)\, \delta i \tag{7.82}$$

$$\delta T^{\mathscr{C}}_{\mathscr{I}\,32} = T^{\mathscr{C}}_{\mathscr{I}\,31}\delta\Omega - (\cos i_0 \cos\Omega_0)\, \delta i \tag{7.83}$$

$$\delta T^{\mathscr{C}}_{\mathscr{I}\,33} = -\sin i_0 \delta i \tag{7.84}$$

Substituting Eq. (7.76) into Eq. (7.75) and equating to Eq. (7.69) gives

$$x = \delta r \tag{7.85}$$

$$y = r_0 \left(\delta\theta + \delta\Omega \cos i_0 \right) \tag{7.86}$$

$$z = r_0 \left(\delta i \sin\theta_0 - \delta\Omega \sin i_0 \cos\theta_0 \right) \tag{7.87}$$

where

$$r_0 = \frac{a_0(1 - e_0^2)}{1 + e_0 \cos f_0} = \frac{a_0 \left(1 - q_{10}^2 - q_{20}^2 \right)}{1 + q_{10} \cos\theta_0 + q_{20} \sin\theta_0} \tag{7.88}$$

$$\begin{aligned} \delta r = {} & \left(\frac{r_0}{a_0} \right) \delta a - 2 r_0 \left(\frac{a_0}{p_0} \right) (q_{10}\delta q_1 + q_{20}\delta q_2) \\ & - \frac{r_0^2}{p_0} \left[\delta q_1 \cos\theta_0 + \delta q_2 \sin\theta_0 + (q_{20} \cos\theta_0 - q_{10} \sin\theta_0)\, \delta\theta \right] \end{aligned} \tag{7.89}$$

Similarly,

$$[\mathbf{v}_1]_{\mathscr{C}} = T_{\mathscr{I}}^{\mathscr{C}} T_{\mathscr{D}}^{\mathscr{I}} \begin{pmatrix} v_{r1} \\ v_{t1} \\ v_{n1} \end{pmatrix}$$

$$[\mathbf{v}_1]_{\mathscr{C}} = T_{\mathscr{I}}^{\mathscr{C}} \left(T_{\mathscr{C}}^{\mathscr{I}} + \delta T_{\mathscr{C}}^{\mathscr{I}} \right) \begin{pmatrix} v_{r0J_2} + \delta v_r \\ v_{t0J_2} + \delta v_t \\ v_{n0J_2} + \delta v_n \end{pmatrix}$$

$$\begin{aligned} [\mathbf{v}_1]_{\mathscr{C}} = & \begin{pmatrix} v_{r0J_2} + \delta v_r \\ v_{t0J_2} + \delta v_t \\ v_{n0J_2} + \delta v_n \end{pmatrix} + v_{r0J_2} \begin{pmatrix} 0 \\ \delta\theta + \delta\Omega_0 \cos i_0 \\ \delta i \sin\theta_0 - \delta\Omega \cos\theta_0 \sin i_0 \end{pmatrix} \\ & + v_{t0J_2} \begin{pmatrix} -\delta\theta - \delta\Omega \cos i_0 \\ 0 \\ \delta i \cos\theta_0 + \delta\Omega \sin\theta_0 \sin i_0 \end{pmatrix} \\ & + v_{n0J_2} \begin{pmatrix} -\delta i \sin\theta_0 + \delta\Omega_0 \cos\theta_0 \sin i_0 \\ -\delta i \cos\theta_0 - \delta\Omega \sin\theta_0 \sin i_0 \\ 0 \end{pmatrix} \end{aligned} \tag{7.90}$$

The velocity components are now divided into two parts: Those not depending directly on J_2 and those depending on J_2. The first part is expressed in terms of the orbital elements, and has the same form as the unperturbed motion. The second part, denoted by Δ, is the variation caused by only J_2:

$$v_{jJ_2} = v_j + \Delta v_j, \quad \delta v_{jJ_2} = \delta v_j + \delta\Delta v_j, \quad j = r, t, n \tag{7.91}$$

From these equations, the relationship between the state $\mathbf{x}(t)$ and $\delta\mathbf{\alpha}(t)$ is

$$\begin{pmatrix} x \\ y \\ z \end{pmatrix} = \begin{pmatrix} \left(\frac{r_0}{a_0}\right) \delta a + \left(\frac{r_0^2}{p_0}\right) (q_{10} \sin\theta_0 - q_{20} \cos\theta_0)\, \delta\theta \\ -\left(\frac{r_0}{p_0}\right) \left[(2a_0 q_{10} + r_0 \cos\theta_0)\, \delta q_1 - (2a_0 q_{20} + r_0 \sin\theta_0)\, \delta q_2 \right] \\ r_0 \left(\delta\theta + \delta\Omega \cos i_0\right) \\ r_0 \left(\delta i \sin\theta_0 - \delta\Omega \sin i_0 \cos\theta_0\right) \end{pmatrix} \tag{7.92}$$

$$\begin{aligned} \begin{pmatrix} \dot{x} \\ \dot{y} \\ \dot{z} \end{pmatrix} = & \begin{pmatrix} \delta v_r \\ \delta v_t \\ \delta v_n \end{pmatrix} + v_{r0} \begin{pmatrix} 0 \\ \delta\theta + \delta\Omega \cos i_0 \\ \delta i \sin\theta_0 - \delta\Omega \sin i_0 \cos\theta_0 \end{pmatrix} \\ & + v_{t0} \begin{pmatrix} -\delta\theta - \delta\Omega \cos i_0 \\ 0 \\ \delta i \cos\theta_0 + \delta\Omega \sin i_0 \sin\theta_0 \end{pmatrix} \\ & + v_{n0} \begin{pmatrix} -\delta i \sin\theta_0 + \delta\Omega \sin i_0 \cos\theta_0 \\ -\delta i \cos\theta_0 - \delta\Omega \sin i_0 \sin\theta_0 \\ 0 \end{pmatrix} \\ & + \begin{pmatrix} \delta\Delta v_r \\ \delta\Delta v_t \\ \delta\Delta v_n \end{pmatrix} + \varpi_{n0} \begin{pmatrix} y \\ -x \\ 0 \end{pmatrix} + \varpi_{r0} \begin{pmatrix} 0 \\ z \\ -y \end{pmatrix} + \varpi_{t0} \begin{pmatrix} -z \\ 0 \\ x \end{pmatrix} \end{aligned}$$

$$
\begin{aligned}
&+\Delta v_{r0}\begin{pmatrix} 0 \\ \delta\theta + \delta\Omega\cos i_0 \\ \delta i\sin\theta_0 - \delta\Omega\sin i_0\cos\theta_0 \end{pmatrix} \\
&+\Delta v_{r0}\begin{pmatrix} 0 \\ \delta\theta + \delta\Omega\cos i_0 \\ \delta i\sin\theta_0 - \delta\Omega\sin i_0\cos\theta_0 \end{pmatrix} \\
&+\delta v_{t0}\begin{pmatrix} -\delta\theta - \delta\Omega\cos i_0 \\ 0 \\ \delta i\cos\theta_0 + \delta\Omega\sin i_0\sin\theta_0 \end{pmatrix}
\end{aligned} \tag{7.93}
$$

The angular velocity for osculating elements is

$$
\begin{aligned}
\boldsymbol{\varpi} = &\left(\dot{\Omega}_0\sin\theta_0\sin i_0 + (\mathrm{d}i_0/\mathrm{d}t)\cos\theta_0\right)\hat{\mathbf{x}} \\
&+\left(\dot{\Omega}_0\cos\theta_0\sin i_0 - (\mathrm{d}i_0/\mathrm{d}t)\sin\theta_0\right)\hat{\mathbf{y}} + \left(\dot{\theta}_0 + \dot{\Omega}_0\cos i_0\right)\hat{\mathbf{z}}
\end{aligned} \tag{7.94}
$$

With osculating elements, the orbit plane is defined by the position and velocity, so the velocity of the chief must be in the reference plane; therefore, the $\hat{\mathbf{z}}$-component of the osculating angular velocity must be zero. This yields

$$
\dot{\Omega}_0\cos\theta_0\sin i_0 = \frac{di_0}{dt}\sin\theta_0 \tag{7.95}
$$

and the osculating angular velocity becomes

$$
\boldsymbol{\varpi} = \left(\dot{\Omega}_0\sin i_0/\sin\theta_0\right)\hat{\mathbf{x}} + \left(\dot{\theta}_0 + \dot{\Omega}_0\cos i_0\right)\hat{\mathbf{z}} \tag{7.96}
$$

The angle rates are needed to obtain the $\Sigma(t)$ matrix. They are obtained from the Hamiltonian, Eqs. (3.10) and (3.18), and the GVE of Section 2.5.4:

$$
\frac{di_0}{dt} = -A_2\left(\frac{n_0}{4a_0^2\eta_0^7}\right)(1 + q_{10}\cos\theta_0 + q_{20}\sin\theta_0)\sin(2i_0)\sin(2\theta_0) \tag{7.97}
$$

$$
\dot{\Omega}_0 = -A_2\left(\frac{n_0}{4a_0^2\eta_0^7}\right)(1 + q_{10}\cos\theta_0 + q_{20}\sin\theta_0)\cos i_0\sin^2\theta_0 \tag{7.98}
$$

The angular momentum perpendicular to the orbit plane provides the last angular rate:

$$
\begin{aligned}
h_0 &= r_0^2\varpi_{n0} = r_0^2\left(\dot{\theta}_0 + \dot{\Omega}_0\cos i_0\right) = \sqrt{\mu p_0} \\
\dot{\theta}_0 &= \sqrt{\frac{\mu}{p_0^3}}(1 + q_{10}\cos\theta_0 + q_{20}\sin\theta_0)^2 - \dot{\Omega}_0\cos i_0
\end{aligned} \tag{7.99}
$$

The velocity components are

$$\begin{aligned} v_{r0} &= \dot{r}_0 = \sqrt{\mu/p_0}\,(q_{10}\sin\theta_0 - q_{20}\cos\theta_0) \\ v_{t0} &= r_0\varpi_{n0} = \sqrt{\mu/p_0}\,(1 + q_{10}\cos\theta_0 + q_{20}\sin\theta_0) \\ v_{n0} &= 0 \\ \Delta v_{j0} &= \delta\Delta v_{j0} = 0, \quad j = r, t, n \end{aligned} \tag{7.100}$$

The last quantities needed are the variations of the velocity components, which are

$$\begin{aligned} \delta v_r = &-\left[\left(\frac{n_0}{2\eta_0^3}\right)\delta a - \left(\frac{3n_0a_0}{\eta_0^4}\right)\delta\eta\right](q_{10}\sin\theta_0 - q_{20}\cos\theta_0) \\ &+\left(\frac{a_0n_0}{\eta_0^3}\right)[\delta q_1\sin\theta_0 - \delta q_2\cos\theta_0 + (q_{10}\cos\theta_0 + q_{20}\sin\theta_0)\,\delta\theta] \end{aligned} \tag{7.101}$$

$$\begin{aligned} \delta v_t = &-\left[\left(\frac{n_0}{2\eta_0^3}\right)\delta a - \left(\frac{3n_0a_0}{\eta_0^4}\right)\delta\eta\right](1 + q_{10}\cos\theta_0 + q_{20}\sin\theta_0) \\ &+\left(\frac{a_0n_0}{\eta_0^3}\right)[\delta q_1\cos\theta_0 + \delta q_2\sin\theta_0 + (-q_{10}\sin\theta_0 + q_{20}\cos\theta_0)\,\delta\theta] \end{aligned} \tag{7.102}$$

Substituting these quantities into Eqs. (7.92) and (7.93) yields the matrices $\Sigma(t)$ and $\Sigma^{-1}(t)$, the elements of which are given in Appendices A and B, respectively.

THE TRANSFORMATION MATRIX $\bar{\Sigma}(t) = [\bar{A}(t) + A_2\bar{B}(t)]$

Since the matrix $A(t)$ is a function of the osculating elements without J_2 effects, it is functionally equal to $\bar{A}(t)$ with mean elements being substituted for osculating elements, that is, $\bar{A} = A(\overline{\mathbf{oe}})$. In addition to mean elements being used, the constraint that the velocity be in the orbit plane no longer applies. Thus, the angular velocity is different and the velocity components affected by J_2 are different. From Eqs. (7.42), the secular angle rates, denoted by the superscript $(\cdot)^{(s)}$, are

$$\frac{\mathrm{d}i_0^{(s)}}{\mathrm{d}t} = 0 \tag{7.103}$$

$$\dot{\Omega}_0^{(s)} = -0.5A_2\left(\frac{n_0}{a_0^2\eta_0^4}\right)\cos i_0 \tag{7.104}$$

$$\dot{\omega}_0^{(s)} = -0.25A_2\left(\frac{n_0}{a_0^2\eta_0^4}\right)\left(1 - 5\cos^2 i_0\right) \tag{7.105}$$

$$\dot{M}_0^{(s)} = n_0 + 0.25A_2\left(\frac{n_0}{a_0^2\eta_0^3}\right)\left(2 - 3\sin^2 i_0\right) \tag{7.106}$$

The mean argument of latitude rate is given by Eq. (7.99), but using $\dot{\Omega}_0^{(s)}$ instead of the osculating rate. The mean angular velocity is

$$\begin{aligned}\overline{\boldsymbol{\omega}} = &\left(\dot{\Omega}_0^{(s)} \sin\theta_0 \sin i_0\right)\hat{\mathbf{x}} + \left(\dot{\Omega}_0^{(s)} \cos\theta_0 \sin i_0\right)\hat{\mathbf{y}} \\ &+ \left(\dot{\theta}_0^{(s)} + \dot{\Omega}_0^{(s)} \cos i_0\right)\hat{\mathbf{z}}\end{aligned} \tag{7.107}$$

The variations of the velocity components due to J_2 are not zero, and are given by

$$\begin{aligned}\Delta v_r &= -\left(\frac{r_0^2}{p_0}\right)(q_{10}\sin\theta_o - q_{20}\cos\theta_0)\,\dot{\omega}_0^{(s)} \\ \Delta v_t &= r_0\dot{\Omega}_0^{(s)}\cos i_0 \\ \Delta v_n &= -r_0\dot{\Omega}_0^{(s)}\sin i_0\cos\theta_0\end{aligned} \tag{7.108}$$

Substituting Eqs. (7.108) and their variation into Eqs. (7.92) and (7.93) gives the matrix $\bar{B}(t)$, whose elements are given in Appendix C.

THE MEAN ELEMENT STATE TRANSITION MATRIX $\bar{\phi}_{\overline{\text{oe}}}$

With only J_2 perturbations, the mean elements are

$$\begin{aligned}&a = a(0), \quad i = i(0), \quad e = e(0) \\ &q_1 = e\cos\omega = q_1(0)\cos\left[\dot{\omega}^{(s)}\,(t-t_0)\right] + q_{20}\sin\left[\dot{\omega}^{(s)}\,(t-t_0)\right] \\ &q_2 = e\sin\omega = q_1(0)\sin\left[\dot{\omega}^{(s)}\,(t-t_0)\right] - q_{20}\cos\left[\dot{\omega}^{(s)}\,(t-t_0)\right] \\ &\Omega = \Omega(0) + \dot{\Omega}^{(s)}\,(t-t_0)\end{aligned} \tag{7.109}$$

Now, define the mean argument of latitude, λ, and the eccentric argument of latitude, F:

$$\lambda = M + \omega, \quad F = E + \omega \tag{7.110}$$

From Kepler's equation, $M = E - e\sin E$ (Eq. (2.26)), the *modified Kepler equation* for λ and F reads

$$\lambda = F - q_1\sin F + q_2\cos F \tag{7.111}$$

From Ref. [75], the relationship between the true and eccentric arguments of latitude is given by

$$\tan F = \frac{r\left(1+\beta q_1^2\right)\sin\theta - \beta q_1 q_2\cos\theta + a q_1}{r\left(1+\beta q_2^2\right)\cos\theta - \beta q_1 q_2\sin\theta + a q_2} \tag{7.112}$$

where

$$\beta = \frac{1}{\left[\left(1-e^2\right)+\sqrt{1-e^2}\right]} = \frac{1}{\eta\left(1+\eta\right)} \tag{7.113}$$

The relationship between λ and θ becomes

$$\lambda = F - \frac{\sqrt{1-q_1^2-q_2^2}\left(q_1 \sin\theta - q_2\, cos\theta\right)}{\left(1+q_1\cos\theta+q_2\sin\theta\right)} \tag{7.114}$$

with F given by Eq. (7.112). Now, define

$$G \equiv \lambda - \lambda(t_0) = M(0)+\omega(0)+\left(\dot{M}^{(s)}+\dot{\omega}^{(s)}\right)(t-t_0) \tag{7.115}$$

We now have all the elements of $\overline{\mathbf{oe}}$ as a function of time. The state transition matrix, $\phi_{\overline{\mathbf{oe}}}(t,t_0)$ of $\delta\overline{\mathbf{oe}}(t)$, is obtained by expanding these equations in a Taylor series about the chief elements, $\overline{\mathbf{oe}}_0(t)$. The elements of $\phi_{\overline{\mathbf{oe}}}(t,t_0)$ are given in Appendix D.

MEAN-TO-OSCULATING TRANSFORMATION

As we have seen in Section 3.4, the first-order mean-to-osculating transformation is given by

$$\mathbf{oe} = \overline{\mathbf{oe}} + \epsilon\left\{\overline{\mathbf{oe}}, W_1\right\} \tag{7.116}$$

where $\left\{\overline{\mathbf{oe}}, W_1\right\}$ is the Poisson bracket. Usually, the mean-to-osculating transformation is performed by two transformations, mean-to-long-periodic using $W_1^{(lp)}$, and then long-periodic-to-osculating using $W_1^{(sp)}$. However, since we are only performing the first-order transformation, it can be performed as a single transformation, and the differences are of $\mathcal{O}(J_2^2)$. For convenience, the short-periodic generating function is separated into two parts: $W_1^{(sp1)}$, which is a function of only the true anomaly, and $W_1^{(sp2)}$, which is a function of the true anomaly and the argument of perigee. From Section 3.4, the generating functions are

$$\begin{aligned} W_1^{(lp)} = &-\left(\frac{1}{32G^3}\right)\left(1-\frac{G^2}{L^2}\right)\left(1-5\frac{H^2}{G^2}\right)^{-1} \\ &\times\left(1-16\frac{H^2}{G^2}+15\frac{H^4}{G^4}\right)\sin 2g \end{aligned} \tag{7.117}$$

and

$$W_1^{(sp1)} = -\frac{1}{4G^3}\left(1-3\frac{H^2}{G^2}\right)\left(f-l+e\sin f\right) \tag{7.118}$$

$$W_1^{(sp2)} = \frac{3}{8G^3}\left(1 - \frac{H^2}{G^2}\right) \times \left[\sin(2f + 2g) + e\sin(f + 2g) + \frac{e}{3}\sin(3f + 2g)\right] \quad (7.119)$$

We define

$$\mathfrak{oe} = \overline{\mathfrak{oe}} - J_2 R_e^2 \left(\mathfrak{oe}^{(lp)} + \mathfrak{oe}^{(sp1)} + \mathfrak{oe}^{(sp2)}\right) \quad (7.120)$$

where

$$\mathfrak{oe}^{(lp)} = \frac{1}{R_e^2}\{W_1^{(lp)}, \overline{\mathfrak{oe}}\} \quad (7.121)$$

$$\mathfrak{oe}^{(sp1)} = \frac{1}{R_e^2}\{W_1^{(sp1)}, \overline{\mathfrak{oe}}\} \quad (7.122)$$

$$\mathfrak{oe}^{(sp2)} = \frac{1}{R_e^2}\{W_1^{(sp2)}, \overline{\mathfrak{oe}}\} \quad (7.123)$$

The generating functions, Eqs. (7.117)–(7.119), depend upon normalized variables. To perform the above Poisson bracket operations, they need to be transformed back to regular variables. The mean-to-osculating transformations for the elements of $\mathfrak{oe}$ are given in Appendix E.

The long-periodic terms appear as secular terms of $\mathcal{O}(J_2^2)$ for periods of time much less than the argument of perigee rotation period, T_{pr}. Since the second-order secular terms have not been considered, the long-periodic terms could probably be dropped in the mean-to-osculating transformation if the prediction time is small compared to T_{pr}, say $0.1T_{pr}$. In addition, note the term $(1 - G^2/L^2) = e^2$ in $W^{(lp)}$. This means that all the long-periodic terms in the mean-to-osculating transformation are multiplied by e or e^2. Therefore, for near-circular orbits, the long-periodic terms in the mean-to-osculating transformation could be ignored.

THE D MATRIX

The D matrix is given by

$$D = \frac{\partial \mathfrak{oe}}{\partial \overline{\mathfrak{oe}}} \quad (7.124)$$

Using Eq. (7.116) we get

$$D = I + \epsilon \frac{\partial\{W_1^{(lp)} + W_1^{(sp1)} + W_1^{(sp2)}, \overline{\mathfrak{oe}}\}}{\partial \overline{\mathfrak{oe}}} \quad (7.125)$$

Define

$$D = I - J_2 R_e^2 \left(D^{(lp)} + D^{(sp1)} + D^{(sp2)}\right) \quad (7.126)$$

where

$$D^{(lp)} = \frac{\partial\{W_1^{(lp)}, \overline{\boldsymbol{\alpha}}\}}{\partial\overline{\boldsymbol{\alpha}}} \tag{7.127}$$

$$D^{(sp1)} = \frac{\partial\{W_1^{(sp1)}, \overline{\boldsymbol{\alpha}}\}}{\partial\overline{\boldsymbol{\alpha}}} \tag{7.128}$$

$$D^{(sp2)} = \frac{\partial\{W_1^{(sp2)}, \overline{\boldsymbol{\alpha}}\}}{\partial\overline{\boldsymbol{\alpha}}} \tag{7.129}$$

The elements of $D^{(lp)}$, $D^{(sp1)}$ and $D^{(sp2)}$ are given in Appendix F.

NUMERICAL EVALUATION

To evaluate the Geometric Method, the predicted relative motion is compared with the results obtained by a numerical integration, performed according to the following stages: (i) integrating the equations of motion for both satellites in an ECI frame with a $J_2 - J_5$ gravity field; (ii) transforming the position and velocity obtained in the ECI frame to the chief LVLH frame; (iii) transforming the position and velocity into the curvilinear frame; and (iv) differencing the position and velocity to obtain the relative state. The initial conditions are chosen such that the projection of the relative orbit in the horizontal plane is a 0.5-km radius circle when the chief orbit is circular with the same semimajor axis. This means that the CW equations will predict a PCO with a radius of 500 m. The out-of-plane motion is created by a differential inclination in order to create secular out-of-plane drift. The eccentricity is chosen to be 0.1. Tables 7.1 and 7.2 give the respective initial conditions of the chief and the deputy, which were selected for the numerical evaluation.

Figure 7.2 shows the three-dimensional relative motion predicted by the CW equations, numerical integration and the Geometric Method for one day. Note

Table 7.1 Chief initial conditions

Element	a (km)	θ (deg)	i (deg)	q_1	q_2	Ω (deg)
Osculating	8500	170	70	9.397×10^{-2}	3.420×10^{-2}	45
Mean	8494.549	170.003	69.9929	9.420×10^{-2}	3.407×10^{-2}	45.006

Table 7.2 Deputy osculating initial conditions

δa (m)	$\delta\theta$ (deg)	δi (deg)	δq_1	δq_2	$\delta\Omega$ (deg)
-103.624	-1.104×10^{-3}	7.076×10^{-4}	4.262×10^{-5}	-9.708×10^{-6}	3.227×10^{-3}
x (m)	y (m)	z (m)	$\dot{x}$ (m/s)	$\dot{y}$ (m/s)	$\dot{z}$ (m/s)
250	0	500	0	-0.403	0

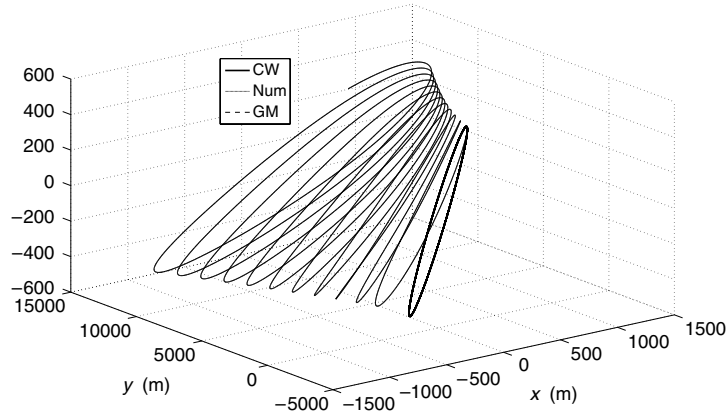

FIGURE 7.2 3D relative trajectory.

that the CW equations predict a periodic trajectory, but the actual motion is much different. To the scale of the figure, the numerical and GM trajectories are the same. Figure 7.3 shows the along-track, radial and out-of-plane time histories. The CW time histories are periodic, because the initial conditions were set up to result in a PCO. As with the 3D plot, the difference in the numerical integration and the GM is not evident with the scale in the plot. Those differences are presented in the next set of plots. The along-track plot shows the secular growth that occurs when not including J_2 and the chief eccentricity in the model. There is out-of-plane secular growth, but over the time period of one day it is only about 10 m, so it does not show up. Thus, the out-of-plane time histories appear equal. The errors in the osculating relative state in the GM are shown in Figs. 7.4 and 7.5. The position errors are less than 2 m and the velocity errors are less than 2 mm/s after one day. The errors in the mean state are shown in Figs. 7.6 and 7.7. The maximum mean state errors are greater than the osculating state errors, because the mean error is based on the true osculating state; thus, the larger mean error is due to the unmodeled short-periodic variations. However, the errors are still small. More detailed error evaluations can be found in Ref. [131].

The mean to osculating transformation (see Appendix E), contains the term $\Theta = \left(1 - 5\cos^2 i\right)^{-1}$. Thus, there is a singularity at $\cos^2 i = 1/5, i = 63.435°, 116.565°$. These inclinations are called the *critical inclinations*. This means that the transformation is not valid near the critical inclination. Figure 7.8 shows the along-track error as a function of the inclination for various values of the eccentricity. The error increases with eccentricity, because the long-periodic terms are multiplied by e or e^2. One can conclude from this figure that there is no problem until the inclination is within 0.2 degrees of the critical inclination. Details on the performance of the GM near the critical inclination are given in Ref. [131]. Theoretically, a new theory needs to be developed. However, what is often done is to set $(1 - 5\cos^2 i) = \varepsilon \text{sign}(1 - 5\cos^2 i)$ whenever $|1 - 5\cos^2 i| < \varepsilon$, where ε is a small number, e.g., 0.05.

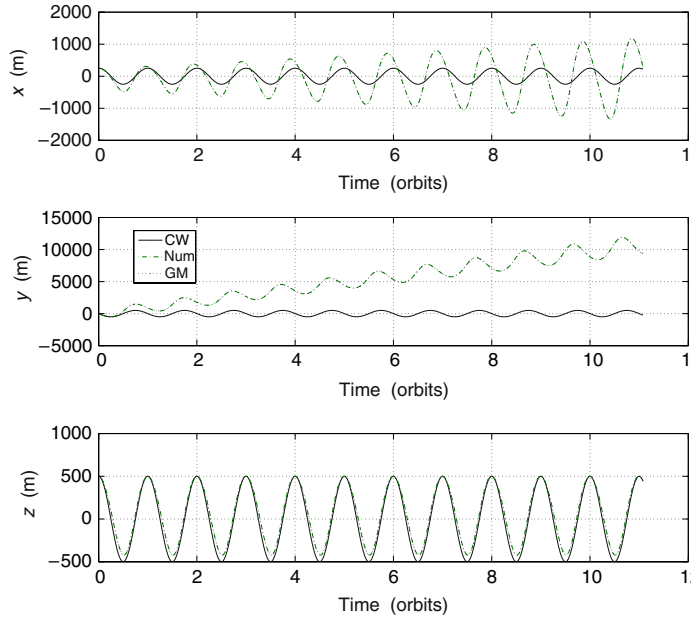

FIGURE 7.3 Position time histories.

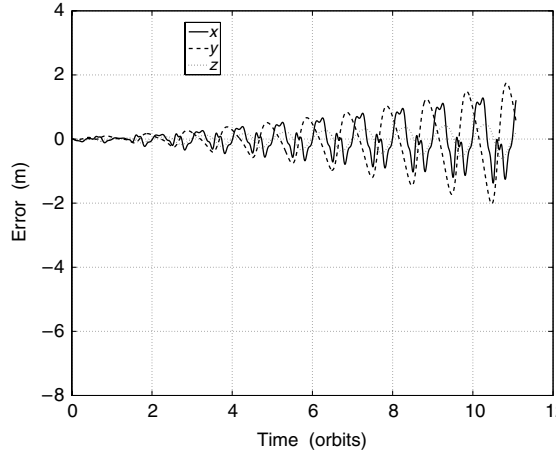

FIGURE 7.4 Geometric method osculating position errors.

7.4 AVERAGED RELATIVE MOTION

The previous developments in this chapter made use of the mean elements extensively. One can, for convenience, define and compute mean motion variables from the differential mean elements instead of the differential osculating elements. However, since the averages of the short-periodic variations in the elements do not necessarily equal zero, errors of $\mathcal{O}(J_2)$ can result due to a

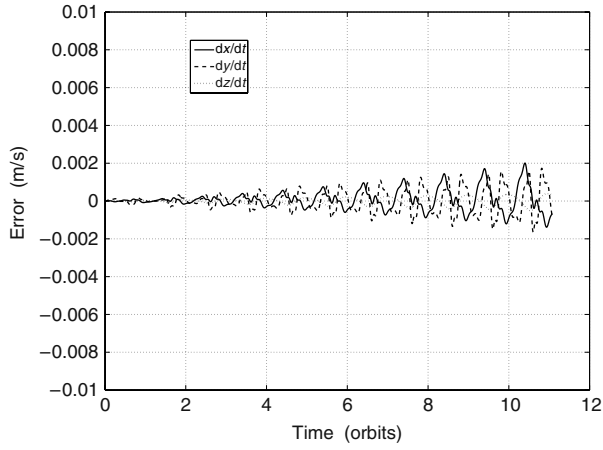

FIGURE 7.5 Geometric method osculating velocity errors.

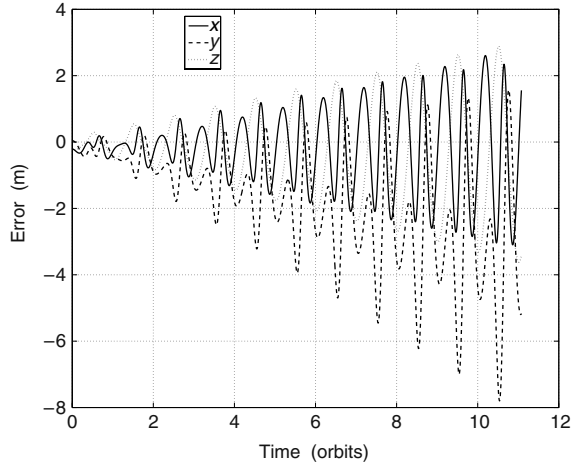

FIGURE 7.6 Geometric method mean position errors.

direct substitution of the differential mean elements into the expressions for the motion variables. Sengupta et al. [125] have obtained corrections to the mean motion variables, resulting in the so-called "averaged" expressions for the relative motion variables. This analytical filtering process of removing the short-periodic oscillations, while simultaneously accounting for their orbit-averaged values, is discussed in this section.

The relationship between the jth osculating element and its short-periodic variation can be written as [132]

$$\mathbf{oe}_j{}^{(sp)} = -J_2 R_e^2 \{\overline{\mathbf{oe}}_j, W^{(sp)}\} \tag{7.130}$$

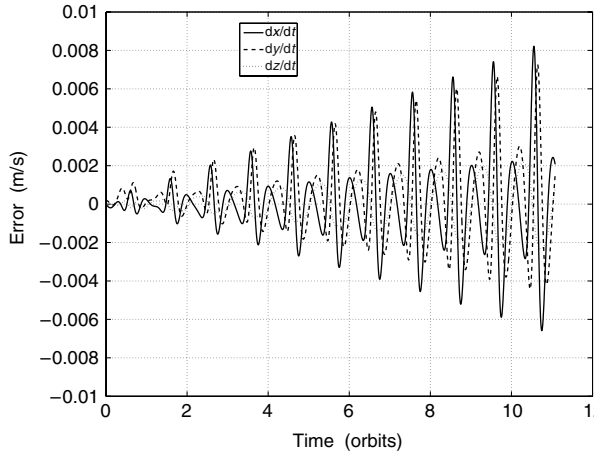

FIGURE 7.7 Geometric method mean velocity errors.

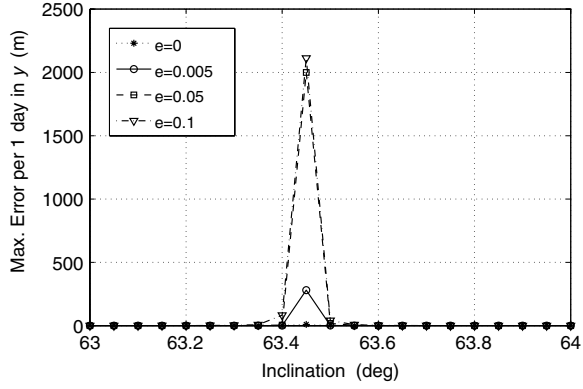

FIGURE 7.8 Along-track errors near the critical inclination.

where $\{\cdot,\cdot\}$ is the Poisson bracket as defined by Eq. (2.93), and $W^{(sp)}$ is the short-periodic generating function (3.22). In a more explicit form, the short-periodic variation of the jth element can be written as

$$\begin{aligned}\boldsymbol{\alpha}_j{}^{(sp)} = -J_2 R_e^2 \Bigg[&\left(\frac{\partial \overline{\boldsymbol{\alpha}}_j}{\partial l}\right)\left(\frac{\partial W^{(sp)}}{\partial L}\right) + \left(\frac{\partial \overline{\boldsymbol{\alpha}}_j}{\partial g}\right)\left(\frac{\partial W^{(sp)}}{\partial G}\right) \\ &+ \left(\frac{\partial \overline{\boldsymbol{\alpha}}_j}{\partial \hbar}\right)\left(\frac{\partial W^{(sp)}}{\partial H}\right) - \left(\frac{\partial \overline{\boldsymbol{\alpha}}_j}{\partial L}\right)\left(\frac{\partial W^{(sp)}}{\partial l}\right) \\ &- \left(\frac{\partial \overline{\boldsymbol{\alpha}}_j}{\partial G}\right)\left(\frac{\partial W^{(sp)}}{\partial g}\right) - \left(\frac{\partial \overline{\boldsymbol{\alpha}}_j}{\partial H}\right)\left(\frac{\partial W^{(sp)}}{\partial \hbar}\right)\Bigg] \end{aligned} \tag{7.131}$$

Sengupta et al. [125] show that Eq. (7.130) can also be used for functions of the mean elements. We present samples of these results here:

$$r^{(sp)} = \bar{a}\,\bar{\eta}^2\left[(1-3\cos^2\bar{i})\left(\frac{\bar{\eta}+\bar{\zeta}}{4(1+\bar{\eta})}+\frac{\bar{\eta}}{2\bar{\zeta}}\right)+\frac{1}{4}\sin^2\bar{i}\,\cos 2\bar{\theta}\right] \tag{7.132a}$$

$$\begin{aligned}\theta^{(sp)} = {} & \frac{\bar{\xi}}{2}-\frac{3}{4}(1-5\cos^2\bar{i})(\bar{\theta}-\bar{\lambda})-\frac{1}{4}(1-3\cos^2\bar{i})\frac{\bar{\xi}}{(1+\bar{\eta})}(\bar{\zeta}+4\bar{\eta}+5)\\ & -\frac{1}{4}\cos^2\bar{i}\,(\bar{q}_1\sin 3\bar{\theta}-\bar{q}_2\cos 3\bar{\theta})+\frac{1}{8}(1-7\cos^2\bar{i})\sin 2\bar{\theta}\\ & +\frac{1}{4}(2-5\cos^2\bar{i})(\bar{q}_1\sin\bar{\theta}+\bar{q}_2\cos\bar{\theta})\end{aligned} \tag{7.132b}$$

where the two new variables ζ and ξ are functions of q_1 and q_2 and are defined as

$$\zeta + j\xi = 1 + (q_1 - j\,q_2)\exp(j\theta) \tag{7.133}$$

and $j = \sqrt{-1}$. Short-periodic corrections are applied to the expressions obtained directly from the mean elements, as shown for the case of r:

$$\bar{r} = \frac{\bar{a}\bar{\eta}^2}{\bar{\zeta}} \tag{7.134a}$$

$$r = \bar{r} + Jr^{(sp)} \tag{7.134b}$$

where

$$J = J_2\left(\frac{R_e}{\bar{a}\bar{\eta}^2}\right)^2$$

The averaged orbital-elements are obtained by adding the orbit averaged short-periodic variations to the respective mean elements, as follows:

$$\widehat{\mathbf{oe}}_j = \overline{\mathbf{oe}}_j + \frac{1}{2\pi}\int_0^{2\pi} \mathbf{oe}_j{}^{(sp)}\,\mathrm{d}M \tag{7.135}$$

where the averaging is performed with respect to the mean anomaly. Equation (7.135) can also be used for any function of the orbital elements. For example, the averaged perturbed radius of a satellite in a mean circular orbit can be obtained from Eqs. (7.132a) and (7.135) as

$$\widehat{r}\,|_{\bar{q}_1=\bar{q}_2=0} = \bar{a}\left[1+\frac{3}{4}J(1-3\cos^2\bar{i})\right] \tag{7.136}$$

In a similar manner, starting with the mean differential element descriptions of the relative motion, Sengupta et al. obtained the following expressions by

averaging the short-periodic effects:

$$\frac{\widehat{x}(t)}{\bar{a}_0} = \left[1 - \frac{3}{4}J\left(1 - 3\cos^2\bar{i}_0\right)\right]\frac{\delta\bar{a}}{\bar{a}_0} - \cos(\bar{\lambda}_0 - \dot{\bar{\omega}}_0 t)\delta\bar{q}_1(0) - \sin(\bar{\lambda}_0 - \dot{\bar{\omega}}_0 t)\delta\bar{q}_2(0) + \frac{9}{4}J\sin 2\bar{i}_0\delta\bar{i} \tag{7.137}$$

$$\begin{aligned}\frac{\widehat{y}(t)}{\bar{a}_0} = &\left[-\frac{3}{2} + \frac{33}{8}J\left(1 - 3\cos^2\bar{i}_0\right)\right](\bar{n}_0 t)\frac{\delta\bar{a}}{\bar{a}_0} \\ &+ \left[1 + \frac{3}{4}J(1 - 3\cos^2\bar{i}_0)\right]\delta\bar{\lambda}(0) \\ &- \frac{21}{4}J\sin 2\bar{i}_0(\bar{n}_0 t)\delta\bar{i} + 2\sin(\bar{\lambda}_0 - \dot{\bar{\omega}}_0 t)\delta\bar{q}_1(0) \\ &- 2\cos(\lambda_0 - \dot{\bar{\omega}}_0 t)\delta\bar{q}_2(0) \\ &+ \left[1 + \frac{3}{4}J\left(1 - 3\cos^2\bar{i}_0\right)\right]\cos\bar{i}_0\delta\bar{\Omega}(0)\end{aligned} \tag{7.138}$$

$$\begin{aligned}\frac{\widehat{z}(t)}{\bar{a}_0} = &-\frac{21}{8}J\sin 2\bar{i}_0\cos\bar{\lambda}_0(\bar{n}_0 t)\frac{\delta\bar{a}}{\bar{a}_0} \\ &+ \left[\sin\bar{\lambda}_0 - \frac{3}{2}J\sin^2\bar{i}_0\cos\bar{\lambda}_0(\bar{n}_0 t)\right]\delta\bar{i} \\ &- \cos\bar{\lambda}_0\sin\bar{i}_0\delta\bar{\Omega}(0) - \frac{3}{4}J\sin 2\bar{i}_0(\delta\bar{q}_1(0) - \delta\bar{q}_2(0))\end{aligned} \tag{7.139}$$

The differences between the averaged and mean-element-based expressions may be small, but are very important nonetheless for long-term *formation maintenance*. An alternative along-track boundedness condition can be derived from Eq. (7.138) for mean circular orbits by setting the secular growth terms therein to zero:

$$\frac{\delta\bar{a}}{\bar{a}_0} = -\frac{7}{2}J_2\left(\frac{R_e}{\bar{a}_0}\right)^2\sin 2\bar{i}_0\delta\bar{i} + \mathcal{O}(J_2^2) \tag{7.140}$$

Equation (7.140) shows that, in general, $\delta a \neq 0$ for locally bounded along-track motion.

7.5 LINEARIZED J_2-DIFFERENTIAL EQUATIONS FOR CIRCULAR ORBITS

In this section, a set of linearized equations for perturbed motion are presented. They are derived by using the mean orbital elements, their mean drift rates due to J_2, and the contributions from the short-periodic effects. A set of nonlinear differential equations for evolving perturbed relative motion dynamics directly in the LVLH frame of the chief has been derived by Kechichian [133]. Kechichian's equations utilize a dragging and precessing reference frame to account for the effects of drag and J_2, and they are quite complex.

The GA STM provides a means for propagating the states (position and velocity vectors) of relative motion for elliptic reference orbits in a curvilinear

coordinate system. However, the expressions for building the STM involve both the short- and long-periodic effects of J_2. The long-periodic terms can be ignored for simplifying the STM, especially for prediction times less than the perigee rotation period and for an $\mathcal{O}(J_2)$ approximation. For mean circular orbits, this is not an approximation, since there are no long-periodic terms in the osculating elements. Hamel and Lafontaine [134] consider such an alternative for propagating the differential orbital elements, but include the short-period effects only for the semimajor axis; they ignore the short-period effects on the other elements. However, since they deal with the classical elements, their fundamental matrix suffers from a singularity for zero mean eccentricity of the reference orbit. Short-periodic corrections to the mean orbital elements for near-circular orbits can be found in Born et al. [135]. Sengupta et al. [125] derive such corrections for elliptic orbits using nonsingular elements. These results have been applied in Ref. [136] for the development of a set of linearized relative motion equations with respect to a mean circular reference orbit. The structure of the model developed is similar to that of Ref. [137], the differences are in the short-periodic approximations utilized. The details of the linear model are presented next.

7.5.1 Development of the model

The relative position vector of a deputy defined in the chief's LVLH frame is denoted by

$$\boldsymbol{\rho} = [x \; y \; z]^T \tag{7.141}$$

and the angular velocity vector of the LVLH frame is

$$\boldsymbol{\omega} = \left[\omega_x \; \omega_y \; \omega_z\right]^T \tag{7.142}$$

with

$$\omega_x = \dot{\Omega}_0 \sin i_0 \sin\theta_0 + \dot{i}_0 \cos\theta_0 \tag{7.143a}$$

$$\omega_y = \dot{\Omega}_0 \sin i_0 \cos\theta_0 - \dot{i}_0 \sin\theta_0 = 0 \tag{7.143b}$$

$$\omega_z = \dot{\Omega}_0 \cos i_0 + \dot{\theta}_0 \tag{7.143c}$$

where Ω_0 is the longitude of the ascending node, θ_0 is the argument of latitude, and i_0 is the inclination of the reference orbit. Equations (7.143a)–(7.143c) involve the osculating elements. The osculating orbit constraint (7.143b) can be verified by substituting the components of $\mathbf{d}$ from Eq. (7.39) into Eqs. (2.107).

The equations of relative motion can be written compactly [137] as

$$\ddot{\boldsymbol{\rho}} = -2\boldsymbol{\omega} \times \dot{\boldsymbol{\rho}} - \boldsymbol{\omega} \times (\boldsymbol{\omega} \times \boldsymbol{\rho}) - \dot{\boldsymbol{\omega}} \times \boldsymbol{\rho} + \nabla F_{g2B} + \nabla F_{gJ_2} \tag{7.144}$$

where ∇F_{g2B} is the gravity gradient acceleration due to the two-body gravity field and ∇F_{gJ_2} is that due to the J_2 potential. The two-body gravity gradient acceleration, expressed in the LVLH frame (see Eqs. (4.14)–(4.16) and

Ref. [106]), is

$$\nabla F_{g2B} = -\mu \begin{bmatrix} \dfrac{(r_0+x)}{[(r_0+x)^2+y^2+z^2]^{\frac{3}{2}}} - \dfrac{1}{r_0^2} \\ \dfrac{y}{[(r_0+x)^2+y^2+z^2]^{\frac{3}{2}}} \\ \dfrac{z}{[(r_0+x)^2+y^2+z^2]^{\frac{3}{2}}} \end{bmatrix} \tag{7.145}$$

where μ is the gravitational parameter and r_0 is the radius of the chief's orbit. Equation (7.145) can be linearized about r_0 to obtain

$$\nabla F_{g2B} \approx -\frac{\mu}{{r_0}^3} \begin{bmatrix} -2x \\ y \\ z \end{bmatrix} \tag{7.146}$$

The linearized J_2 differential acceleration vector, obtained from Eq. (7.39), is [137]

$$\nabla F_{gJ_2} = \Upsilon \begin{bmatrix} 1-3\mathrm{s}_{i_0}^2\mathrm{s}_{\theta_0}^2 & \mathrm{s}_{i_0}^2\mathrm{s}_{2\theta_0} & \mathrm{s}_{2i_0}\mathrm{s}_{\theta_0} \\ \mathrm{s}_{i_0}^2\mathrm{s}_{2\theta_0} & \mathrm{s}_{i_0}^2\left(\frac{7}{4}\mathrm{s}_{\theta_0}^2-\frac{1}{2}\right)-\frac{1}{4} & -\frac{1}{4}\mathrm{s}_{2i_0}\mathrm{c}_{\theta_0} \\ \mathrm{s}_{2i_0}\mathrm{s}_{\theta_0} & -\frac{1}{4}\mathrm{s}_{2i_0}\mathrm{c}_{\theta_0} & \mathrm{s}_{i_0}^2\left(\frac{5}{4}\mathrm{s}_{\theta_0}^2+\frac{1}{2}\right)-\frac{3}{4} \end{bmatrix} \boldsymbol{\rho} \tag{7.147}$$

where s and c stand for sin and cos, respectively and

$$\Upsilon = 6J_2\left(\frac{\mu {R_e}^2}{{r_0}^5}\right)$$

7.5.2 Short-periodic effects

The relationships between the osculating and mean elements for mean circular orbits can be obtained from the detailed expressions given in Ref. [132]. These expressions are also available in Ref. [125] in a convenient form. The relevant variables for the case of circular orbits, derived from those given in Ref. [125], are

$$r_0 = \bar{a}_0\left[1 + J\left\{\frac{3}{4}(1-3\cos^2\bar{i}_0) + \frac{1}{4}\sin^2\bar{i}_0\ \cos 2\overline{\theta}_0\right\}\right] \tag{7.148a}$$

$$\theta_0 = \overline{\theta}_0(0) + \dot{\overline{\theta}}_0 t + \frac{1}{8}J(1-7\cos^2\bar{i}_0\ )\sin 2\overline{\theta}_0 \tag{7.148b}$$

$$i_0 = \bar{i}_0 + \frac{3}{8}J\sin 2\bar{i}_0\cos 2\overline{\theta}_0 \tag{7.148c}$$

$$\Omega_0 = \overline{\Omega}_0(0) + \dot{\overline{\Omega}}_0 t + \frac{3}{4}J\cos\bar{i}_0\sin 2\overline{\theta}_0 \tag{7.148d}$$

where $\overline{\theta}_0 = \overline{\theta}_0(0) + \dot{\overline{\theta}}_0 t$, $J = J_2(\frac{R_e}{\overline{a}_0})^2$, and

$$\dot{\overline{\theta}}_0 = n_0 \left[1 - \frac{3}{2} J (1 - 4\cos^2 \overline{i}_0) \right] \tag{7.149a}$$

$$\dot{\overline{\Omega}}_0 = -\frac{3}{2} J n_0 \cos \overline{i}_0 \tag{7.149b}$$

Substitution of Eqs. (7.148b)–(7.149b) into Eqs. (7.143a)–(7.143c) and the approximation $\theta_0 \approx \overline{\theta}_0$ in the evaluation of the trigonometric functions therein, results in the following expressions for the angular velocities:

$$\omega_x = 2\dot{\overline{\Omega}}_0 \sin \overline{i}_0 \sin \overline{\theta}_0 \tag{7.150a}$$

$$\omega_y = 0 \tag{7.150b}$$

$$\omega_z = \dot{\overline{\Omega}}_0 \cos \overline{i}_0 + \dot{\overline{\theta}}_0 + \frac{1}{4} J n_0 \cos 2\overline{\theta}_0 \sin^2 \overline{i}_0 \tag{7.150c}$$

The mean element approximation is performed by setting $\dot{\Omega}_0 = \dot{\overline{\Omega}}_0$, $\dot{\theta}_0 = \dot{\overline{\theta}}_0$, and $\dot{i}_0 = 0$ in Eqs. (7.143a)–(7.143c). Note that the ω_x expressions, with and without accounting for the short-periodic variations, differ by a factor of two. Equation (7.150b) shows that the approximations developed in this section satisfy the osculating orbit condition Eq. (7.143b). The short-periodic correction to the mean ω_z is obvious from Eq. (7.150c).

7.5.3 The linear model

The relative motion equations are assembled in a matrix form by substituting the relevant expressions derived above into Eq. (7.144), including the linear approximation to ∇F_{g2B} given by Eq. (7.146). The linear model [138] is

$$\begin{bmatrix} \dot{\boldsymbol{\rho}} \\ \ddot{\boldsymbol{\rho}} \end{bmatrix} = \begin{bmatrix} 0 & 0 & 0 & 1 & 0 & 0 \\ 0 & 0 & 0 & 0 & 1 & 0 \\ 0 & 0 & 0 & 0 & 0 & 1 \\ a_{41} & a_{42} & a_{43} & 0 & 2\omega_z & 0 \\ a_{51} & a_{52} & a_{53} & -2\omega_z & 0 & 2\omega_x \\ a_{61} & a_{62} & a_{63} & 0 & -2\omega_x & 0 \end{bmatrix} \begin{bmatrix} \boldsymbol{\rho} \\ \dot{\boldsymbol{\rho}} \end{bmatrix} \tag{7.151}$$

where

$$a_{41} = {\omega_z}^2 + 2\frac{\mu}{{r_0}^3} + \Upsilon(1 - 3\sin^2 \overline{i}_0 \sin^2 \overline{\theta}_0) \tag{7.152a}$$

$$a_{42} = \dot{\omega}_z + \Upsilon(\sin^2 \overline{i}_0 \sin 2\overline{\theta}_0) \tag{7.152b}$$

$$a_{43} = -\omega_x \omega_z + \Upsilon(\sin 2\overline{i}_0 \sin \overline{\theta}_0) \tag{7.152c}$$

$$a_{51} = -\dot{\omega}_z + \Upsilon(\sin^2 \overline{i}_0 \sin 2\overline{\theta}_0) \tag{7.152d}$$

$$a_{52} = {\omega_x}^2 + {\omega_z}^2 - \frac{\mu}{{r_0}^3} + \Upsilon\left[-\frac{1}{4} + \sin^2 \overline{i}_0 \left(\frac{7}{4} \sin^2 \overline{\theta}_0 - \frac{1}{2} \right) \right] \tag{7.152e}$$

$$a_{53} = \dot{\omega}_x + \Upsilon\left(-\frac{1}{4}\sin 2\bar{i}_0 \cos\bar{\theta}_0\right) \tag{7.152f}$$

$$a_{61} = -\omega_x\omega_z + \Upsilon(\sin 2\bar{i}_0 \sin\bar{\theta}_0) \tag{7.152g}$$

$$a_{62} = -\dot{\omega}_x + \Upsilon\left(-\frac{1}{4}\sin 2\bar{i}_0 \cos\bar{\theta}_0\right) \approx 0 \tag{7.152h}$$

$$a_{63} = {\omega_x}^2 - \frac{\mu}{{r_0}^3} + \Upsilon\left[-\frac{3}{4} + \sin^2\bar{i}_0\left(\frac{5}{4}\sin^2\bar{\theta}_0 + \frac{1}{2}\right)\right] \tag{7.152i}$$

Equations (7.152) can be simplified further by making several approximations. For example, it can be shown that $a_{62} \approx 0$ to $\mathcal{O}(J_2)$. The variable y is sensitive to the term a_{53}, especially for initial conditions corresponding to a nonzero nodal difference between the two satellites, i.e., $\delta\Omega(0) \neq 0$. This shows the existence of a coupling between cross-track and in-track variables for certain initial conditions. Another observation is that the terms involving $\mu/{r_0}^3$ in Eq. (7.152) can be reduced by using a binomial expansion of $\mathcal{O}(J_2)$. However, this simplification increases the motion propagation errors over the long run, leading to the conclusion that where possible, terms of $\mathcal{O}({J_2}^2)$ and higher should be retained.

We shall now illustrate the fidelity of the linear model by presenting several examples. Let the reference orbit have the following initial mean nonsingular orbital elements:

$$\bar{a}_0 = 7100 \text{ km}, \quad \bar{\theta}_0 = 0, \quad \bar{i}_0 = 70^\circ$$
$$\bar{q}_{10} = 0, \quad \bar{q}_{20} = 0, \quad \bar{\Omega}_0 = 45^\circ$$

The deputy is set up in a PCO in the examples considered in this section. The initial conditions for setting up such a relative orbit, parameterized by ρ and α, are obtained from Eqs. (6.69) and (7.140) (see also Refs. [1,139]).

Example 7.3. *The following initial conditions on the state variables are obtained for a PCO with* $\rho = 0.5$ km *and* $\alpha = 0$*:*

$$\boldsymbol{\rho}(0) = \begin{bmatrix}-0.000288947081 & 0.500033326318 & 0.000175666681\end{bmatrix}^T \text{ km}$$
$$\dot{\boldsymbol{\rho}}(0) = \begin{bmatrix}0.000263388377 & 0.000000272412 & 0.000527371445\end{bmatrix}^T \text{ km/s}$$

The corresponding initial conditions of the chief and deputy in the ECI frame are

$$\mathbf{r}_0(0) = \begin{bmatrix}5023.558528005 & 5023.558528005 & 0\end{bmatrix}^T \text{ km}$$
$$\mathbf{v}_0(0) = \begin{bmatrix}-1.810956397226 & 1.810956397226 & 7.041120373157\end{bmatrix}^T \text{ km/s}$$
$$\mathbf{r}_1(0) = \begin{bmatrix}5023.437579954 & 5023.679067423 & 0.469973680\end{bmatrix}^T \text{ km}$$
$$\mathbf{v}_1(0) = \begin{bmatrix}-1.810792589537 & 1.810419297938 & 7.041300610075\end{bmatrix}^T \text{ km/s}$$

The errors, in the three components of $\boldsymbol{\rho}$, between the linear and the nonlinear simulation results, are shown in Fig. 7.9. The radial and cross-track errors are slightly biased but are predominantly periodic, unlike the in-track error. The in-track drift rate, $\dot{y}$, estimated from Fig. 7.9, is -11 m in 15 orbits of the chief. The drift predicted by Eq. (5.64) for the data of this example is -11.2 m in 15 orbits. Hence, the in-track drift seen from Fig. 7.9 is predominantly due to the linearization of the two-body relative gravitational acceleration.

Example 7.4. *The initial conditions for this example are for* $\rho = 0.5$ km *and* $\alpha = 90^o$*:*

$$\boldsymbol{\rho}(0) = \begin{bmatrix} 0.250014418391 & 0.000198338483 & 0.500288022195 \end{bmatrix}^T \text{ km}$$
$$\dot{\boldsymbol{\rho}}(0) = \begin{bmatrix} -0.000000124335 & -0.000527557529 & -0.000000019840 \end{bmatrix}^T \text{ km/s}$$

The corresponding initial conditions of the deputy in the ECI frame are

$$\mathbf{r}_1(0) = \begin{bmatrix} 5024.067715322 & 5023.402914470 & 0.171195964 \end{bmatrix}^T \text{ km}$$
$$\mathbf{v}_1(0) = \begin{bmatrix} -1.810892863426 & 1.810892391776 & 7.040872374521 \end{bmatrix}^T \text{ km/s}$$

Figure 7.10 shows that except for a change in the in-track drift rate, the error profiles are quite similar to those seen for the previous example. The radial error is oscillatory with a small superimposed linear growth rate. The in-track drift rate estimated from Fig. 7.10 is -3.5 m in 15 orbits, compared to -3.73 m during the same period, predicted by Eq. (5.64).

Example 7.5. *A PCO with* $\rho = 1$ km *is considered to show the effects of the size of the relative orbit on the model errors.*

Figures 7.11 and 7.12, respectively, show the errors between the linear and nonlinear simulations for $\alpha = 0^\circ$ and $\alpha = 90^\circ$. The errors increase with the size of the relative orbit. The amplitudes of the radial and cross-track errors, as well as the in-track growth rate, show quadratic relationships with ρ for $\alpha = 0^\circ$, as is to be expected from Eq. (5.64). The quadratic relationships of the error amplitudes with ρ are not well satisfied for $\alpha = 90^\circ$, showing a more dominant J_2-effect for this case.

Example 7.6. *The extent of the errors, solely due to the approximation of the* J_2 *disturbance, can be ascertained by replacing the linear two-body differential gravitational acceleration of Eq. (7.146) by the difference of the two-body accelerations for the deputy and the chief given by Eq. (7.145). The effect of this change is evaluated for the* 1 km *PCO considered previously.*

Figure 7.13 shows the errors in the states with respect to the nonlinear simulation results for $\alpha = 0^\circ$ and Fig. 7.14 shows the same for $\alpha = 90^\circ$. The in-track error due to the approximation of the J_2-effect is more for $\alpha = 90^\circ$ as compared to the case of $\alpha = 0$, corroborating the conclusion drawn previously. However, the secular effect due to the J_2-approximation is

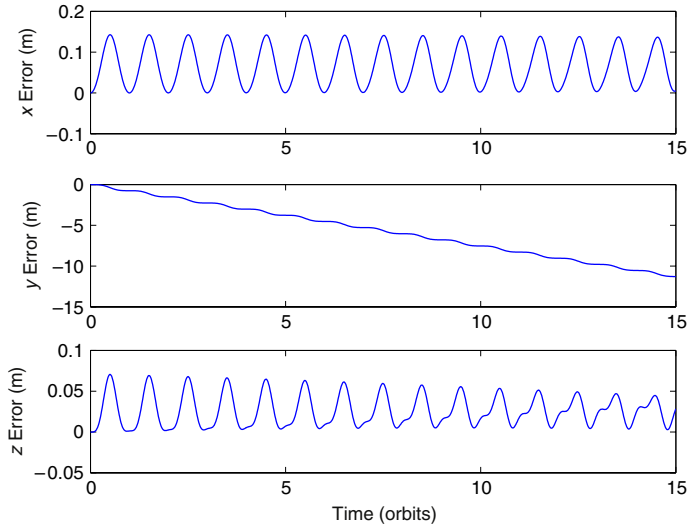

FIGURE 7.9 Errors between the linear and nonlinear models ($\rho = 0.5$ km, $\alpha = 0°$).

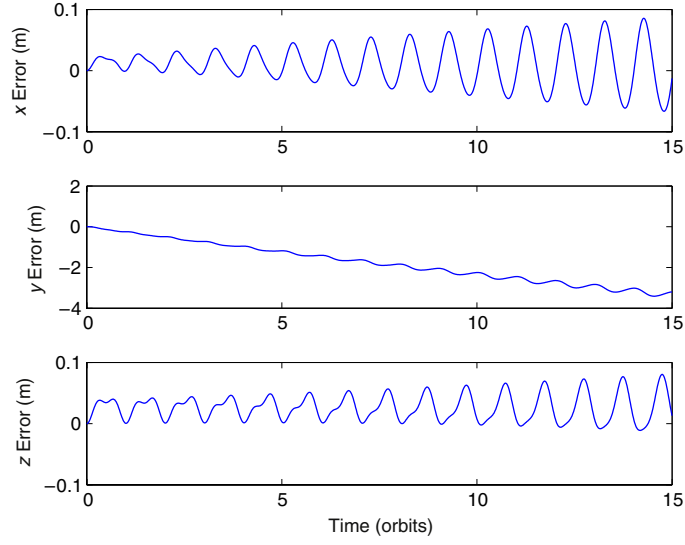

FIGURE 7.10 Errors between the linear and nonlinear models ($\rho = 0.5$ km, $\alpha = 90°$).

very small compared to that due to linearization of the two-body differential gravitational acceleration.

The examples considered in this section show that the linear model is accurate to $\mathcal{O}(J_2)$ and is also consistent with respect to the errors expected from linearization.

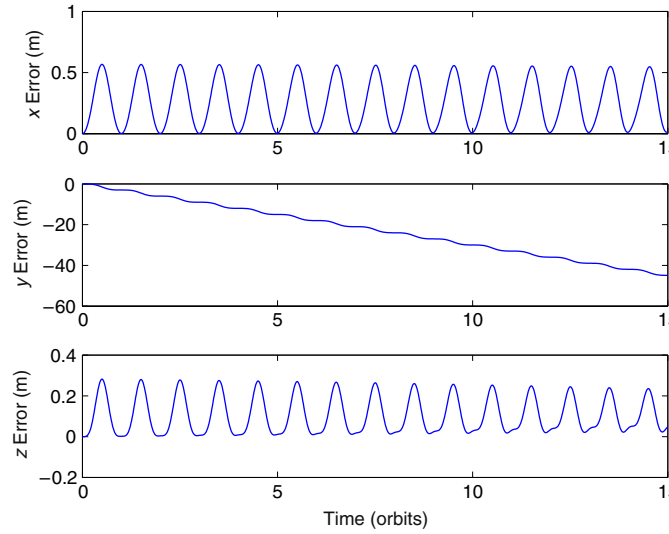

FIGURE 7.11 Errors between the linear and nonlinear models ($\rho = 1$ km, $\alpha = 0°$).

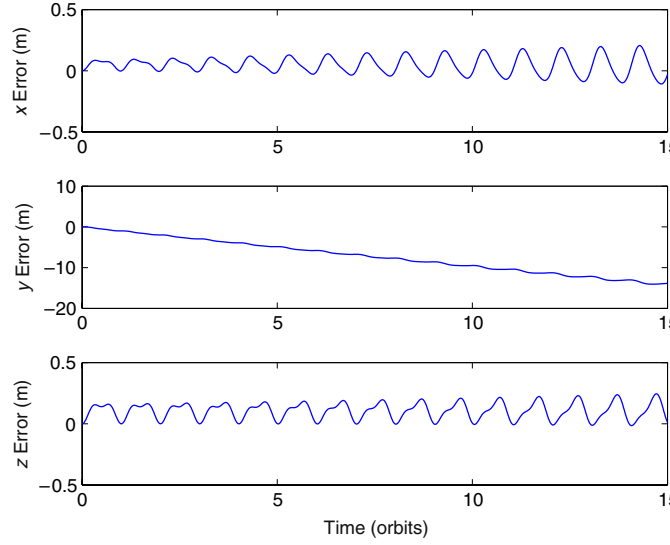

FIGURE 7.12 Errors between the linear and nonlinear models ($\rho = 1$ km, $\alpha = 90°$).

7.6 DIFFERENTIAL EQUATIONS FROM THE GIM–ALFRIEND STM

In principle, a set of linear differential equations can be derived for a dynamical system from its STM. However, the process can be complicated, especially for perturbed eccentric orbits. Simplifications can be achieved by neglecting the long-periodic effects [125,134]. There are no long-periodic effects of the

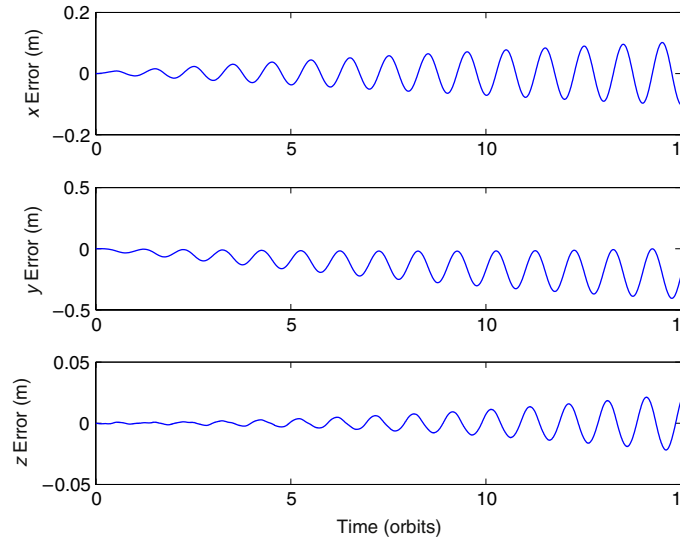

FIGURE 7.13 Errors between the linear-J_2-nonlinear two-body gravitational acceleration model and nonlinear simulation ($\rho = 1$ km, $\alpha = 0°$).

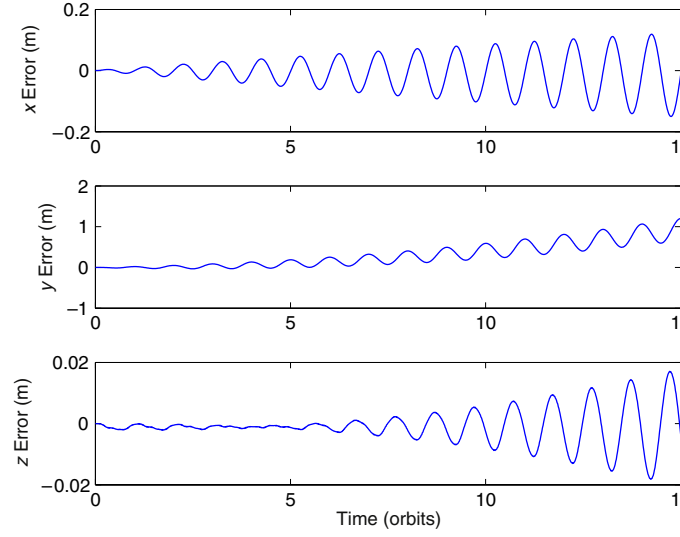

FIGURE 7.14 Errors between the linear-J_2-nonlinear two-body gravitational acceleration model and nonlinear simulation ($\rho = 1$ km, $\alpha = 90°$).

J_2 perturbation on the elements of a mean circular orbit. However, the partial derivatives of the long-periodic correction terms with respect to $\bar{q}_1$ and $\bar{q}_2$ are not zero. These partial derivatives of the long-periodic terms are significant near the critical inclination.

The relationship between the relative state vector and the osculating or mean differential orbital elements at any instant can be written as

$$\mathbf{x}(t) = \Sigma(t)\delta\mathbf{oe}(t) = \Sigma(t)D\delta\overline{\mathbf{oe}}(t) = F_1\delta\overline{\mathbf{oe}}(t) \tag{7.153}$$

where $F_1 = \Sigma(t)D$. The matrix D is the partial derivative matrix of the osculating elements with respect to the mean elements. The elements of $\Sigma(t)$ and D have been derived in Ref. [132] and are also provided in Appendix G for orbits with small eccentricity, but with terms of $\mathcal{O}(eJ_2)$ neglected. The relationship between the current and the initial differential mean elements, either nonsingular or equinoctial, can also be expressed as

$$\delta\overline{\mathbf{oe}}(t) = \bar{\phi}_{\overline{\mathbf{oe}}}(t, t_0)\delta\overline{\mathbf{oe}}(0) \tag{7.154}$$

where $\bar{\phi}_{\overline{\mathbf{oe}}}$ is the state transition matrix for propagating the mean differential elements, which can be obtained from Appendix G. Thus, the relationship between the current relative state and the initial differential mean element vector can be expressed as

$$\mathbf{x}(t) = F_1\bar{\phi}_{\overline{\mathbf{oe}}}(t, t_0)\delta\overline{\mathbf{oe}}(0) = F\delta\overline{\mathbf{oe}}(0) \tag{7.155}$$

where $F = F_1\bar{\phi}_{\overline{\mathbf{oe}}}(t, t_0)$. Since $\delta\overline{\mathbf{oe}}(0)$ is a constant vector, an approach to obtain a linear state-space model is to differentiate Eq. (7.155) and eliminate $\delta\overline{\mathbf{oe}}(0)$:

$$\dot{\mathbf{x}}(t) = \dot{F}F^{-1}\mathbf{x}(t) \tag{7.156}$$

Determination of the derivatives of the entries of F is a tedious process for elliptic orbits. The algebra involved is simpler for circular orbits. However, the approach discussed above results in a model that has the same accuracy as that given by Eq. (7.151), since expressing the initial mean differential elements in terms of the current states introduces significant linearization errors. A better approach is outlined next.

Differentiation of Eq. (7.153) and simple variable elimination leads to

$$\dot{\mathbf{x}}(t) = \dot{F}_1\delta\overline{\mathbf{oe}}(t) + F_1\delta\dot{\overline{\mathbf{oe}}}(t) = \dot{F}_1{F_1}^{-1}\mathbf{x}(t) + F_1\dot{\bar{\phi}}_{\bar{e}}(t, t_0)\delta\overline{\mathbf{oe}}(0) \tag{7.157}$$

Equation (7.157) is nonhomogeneous due to the appearance of a reference input that depends on $\delta\overline{\mathbf{oe}}(0)$. Note the similarity of structures between Eqs. (6.76)–(6.78) and Eq. (7.157); these are hybrid equations, involving the position and velocity states as well as the initial differential orbital elements.

Note that for circular orbits all the periodic terms in D are functions of $\overline{\theta}_0$ and hence the derivative of D is easily obtained. The singularity associated with the computation of D near the critical inclination can be avoided by using the limiting procedure given in Section 7.3.2.

The state variable propagation errors due to the use of Eq. (7.157) are shown for $\rho = 1$ km in Figs. 7.15 and 7.16, for $\alpha = 0°$ and $\alpha = 90°$, respectively, and for the initial elements of the chief considered in Section 7.5.

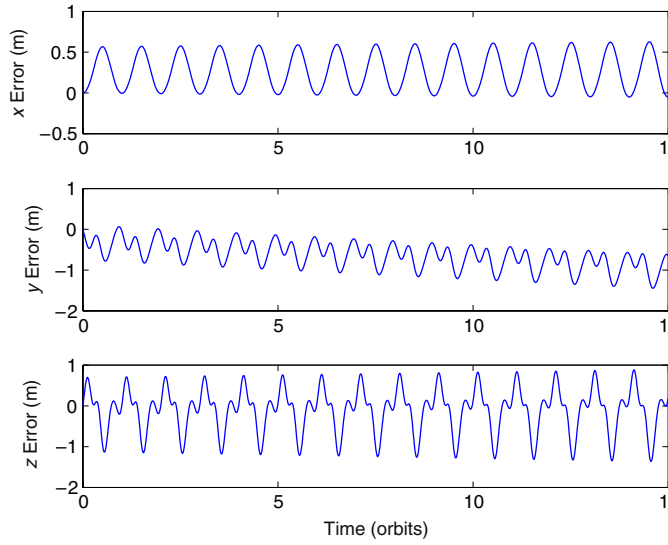

FIGURE 7.15 Errors between the STM-based model and nonlinear propagations ($\rho = 1$ km, $\alpha = 0°$).

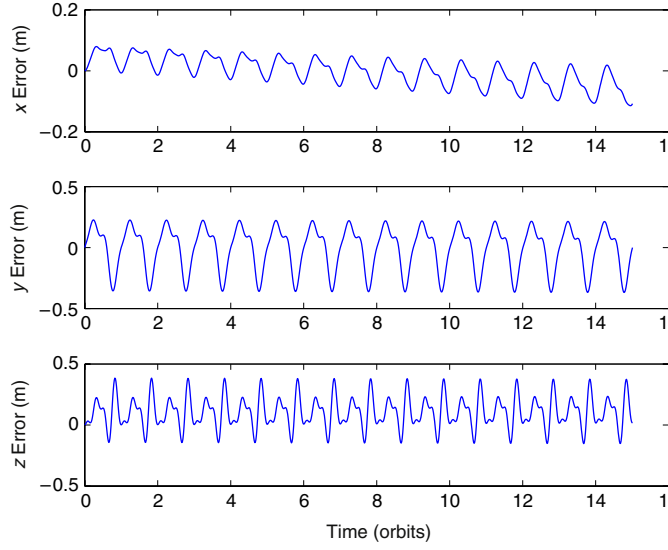

FIGURE 7.16 Errors between the STM-based and nonlinear propagations ($\rho = 1$ km, $\alpha = 90°$).

It is observed by comparing Figs. 7.11 and 7.15 that the secular in-track error has been eliminated considerably by the STM-based hybrid model. There is no appreciable difference between the radial errors from the two models to the scale of the figure. It is remarkable that the cross-track error amplitude from the

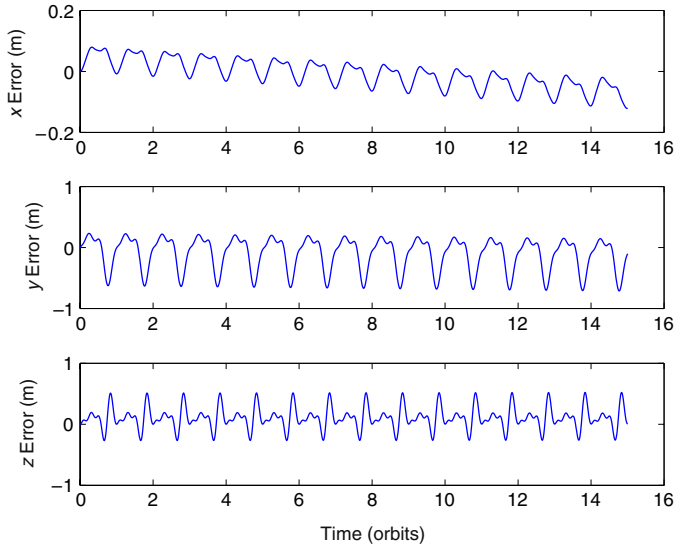

FIGURE 7.17 Errors between the short-periodic-only-STM-based and nonlinear propagations ($\rho = 1$ km, $\alpha = 90°$, and critical inclination).

state-space linearized model is less than that for the STM-based model. Similar observations apply to Figs. 7.12 and 7.16.

There are no appreciable differences in the errors by including or neglecting the long-periodic effects in D, for the examples considered in this section and for the levels of accuracy expected from a first-order theory. In fact, for the critical inclination, neglecting the long-periodic terms results in the errors shown in Fig. 7.17.

7.7 A SECOND-ORDER STATE PROPAGATION MODEL

A second-order state transition approach for propagating perturbed relative motion about eccentric orbits has been proposed by Sengupta et al. [2]. It models the nonlinearities occurring in the unperturbed problem to second order and couples this development with the first-order GA STM, to account for the J_2 perturbation. The main result of this work is the nonlinear propagation equation for the normalized relative motion states with θ as the independent variable:

$$\bar{\mathbf{x}}(\theta_2) = \Phi^{(1)}(\theta_2, \theta_1)\bar{\mathbf{x}}(\theta_1) + \frac{1}{2}\Phi^{(2)}(\theta_2, \theta_1) \otimes \bar{\mathbf{x}}(\theta_1) \otimes \bar{\mathbf{x}}(\theta_1) \qquad (7.158)$$

where θ_1 and θ_2 define the propagation domain, $\Phi^{(1)}$ is the first-order STM, and $\Phi^{(2)}$ is a third-order tensor; $\otimes$ indicates the tensor product. The relative state vector is indicated by $\bar{\mathbf{x}} = \left[\bar{x}, \bar{x}', y, \bar{y}', z, \bar{z}'\right]^T$. The development of Eq. (7.158) is based on a second-order propagation of the mean differential elements and a series reversion process to determine the mean differential elements at any

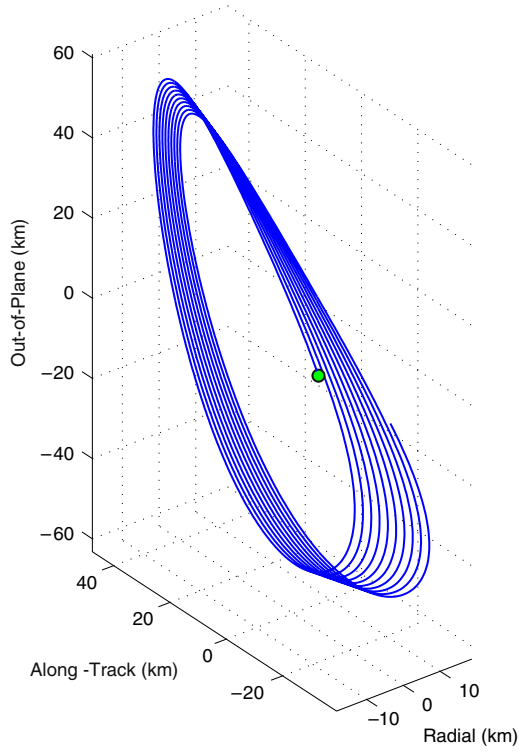

FIGURE 7.18 Relative motion trajectory (adapted from Ref. [2]).

epoch, given the relative state at this time. An example [2] showing the accuracy of the second-order approach is presented next.

Example 7.7. *Let the initial mean elements of the chief be*

$$\bar{a}_0 = 13000 \text{ km}, \quad \bar{\theta}_0 = 0.1 \text{ rad}, \quad \bar{i}_0 = 0.87266 \text{ rad}$$
$$\bar{q}_{10} = 0.29886, \quad \bar{q}_{20} = 0.02615, \quad \bar{\Omega}_0 = 0.34907 \text{ rad}$$

Simulate the evolution of the error in the relative separation distance between the chief and deputy for the initial differential mean elements given below using first- and second-order theories:

$$\delta\bar{a} = 0.2 \text{ km}, \quad \delta\bar{\theta}_0 = -0.15526 \times 10^{-2} \text{ rad}, \quad \delta\bar{i}_0 = 0.005 \text{ rad}$$
$$\delta\bar{q}_{10} = 0.11452 \times 10^{-3}, \quad \delta\bar{q}_{20} = 0.13415 \times 10^{-2}, \quad \delta\bar{\Omega}_0 = 0.2 \times 10^{-3} \text{ rad}$$

Figure 7.18 shows the relative motion trajectory for this example. The errors resulting from the application of the linear and second-order theories are shown in Fig. 7.19 for 10 orbit periods of the chief. The truth model is a nonlinear numerical simulation including J_2. The linear theory results in a final position error of nearly 200 m, whereas the second-order theory reduces the error by one

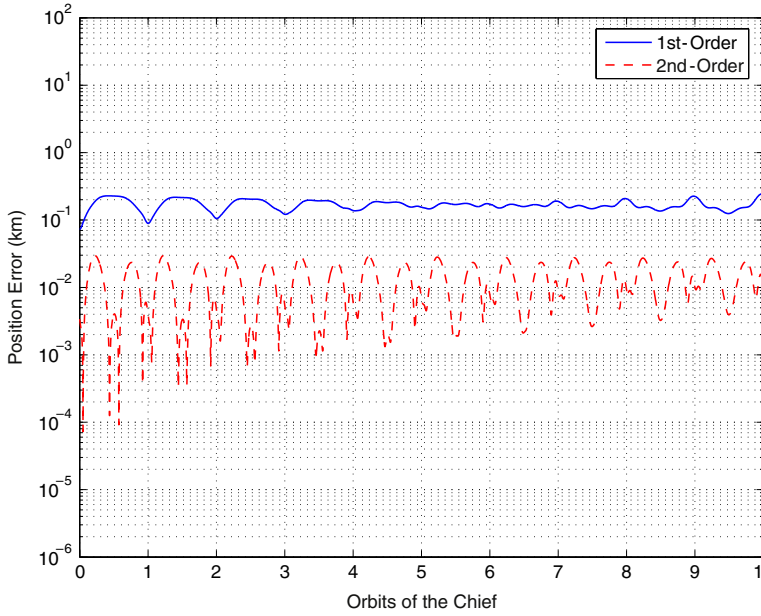

FIGURE 7.19 Position errors resulting from the application of linear and second-order theories (adapted from Ref. [2]).

order of magnitude. For the example considered, the eccentricity and nonlinear effects contribute more significantly to the error than does J_2.

SUMMARY

In this chapter, we discussed the effects of the J_2 perturbation on the orbital elements via the Brouwer Theory. Brouwer's transformation between the mean and osculating orbital elements plays a significant role in the developments in Chapters 8 and 10. We presented the unit-sphere approach to the analytical propagation of relative motion via differential orbital elements and differential Euler parameters.

The GA STM, derived based on the Geometric Method, was developed for nonsingular elements. This STM is valid for any eccentricity and includes the first-order absolute and differential J_2 effects. The relative state used curvilinear coordinates to mitigate the effects of the neglected nonlinear terms that occur when using a relative Cartesian state. The GA STM has been derived for both osculating and mean elements. The mean element version is less accurate, because it does not include the J_2 short-periodic terms, but the secular effects are captured and it is much less complex. The GA STM was developed using the relationship between the relative state in curvilinear coordinates and nonsingular differential orbital elements.

The GA STM presented herein used nonsingular variables for representing the eccentricity. It is not valid near $i = 0$. For the small-inclination case, another

STM had been developed using equinoctial variables. The theory and results can be found in Refs. [100] and [131].

The concept of averaged elements was introduced by accounting for the orbit-averaged short-periodic corrections to the mean elements. The short-periodic corrections to the mean orbital elements were utilized in the development of a consistent set of linearized differential equations for perturbed relative motion. The GA STM can be incorporated into a second-order state transition method to achieve higher levels of accuracy.

A nonlinear relative motion theory due to Yan and Alfriend including J_2^2 terms is discussed in Section 8.2. Several other approaches not discussed in this book account for luni-solar and higher-order geopotential perturbations [140] and use more detailed propagation models such as the Draper Semianalytic Satellite Theory [21] and symplectic integration [141]. Wiesel [142] presents a solution process for relative motion based on the Hamiltonian approach and Floquet theory. The reference orbit for describing relative motion dynamics is a near-circular periodic orbit defined in a nodal frame which regresses about the polar axis of the $\mathscr{I}$ frame.